Modelling Equities with a Stochastic Volatility Jump Diffusion

Matthew Gorven

A dissertation submitted to the Faculty of Commerce, University of Cape Town, in partial fulfilment of the requirements for the degree of Master of Philosophy.

September 16, 2018

MPhil in Mathematical Finance,
University of Cape Town.

Declaration

I declare that this dissertation is my own, unaided work. It is being submitted for the Degree of Master of Philosophy to the University of Cape Town. It has not been submitted before for any degree or examination to any other university.

Matthew Gorven

September 16, 2018

Abstract

The Bates model provides a parsimonious fit to implied volatility surfaces, and its usefulness in developed markets is well documented. However, there is a lack of research assessing its applicability to developing markets. Additionally, research surrounding its usefulness for hedging long term liabilities is limited, despite its frequent use for this purpose.

This dissertation dissects the dynamics of the Bates model into the Heston and Merton models in order to separately examine the effects of stochastic volatility and jumps. Challenges surrounding application of this model are investigated through an evaluation of risk-neutral calibration and simulation methods. The model's ability to fit the implied volatility surfaces from the JSE Top 40 equity index is analysed. Lastly, an evaluation of the model's delta and vega hedging performance is presented by comparing it to the hedge performance of other commonly used models.

Acknowledgements

Firstly, I would like to thank my internal supervisors, Obeid Mahomed and Professor David Taylor for their guidance over the course of this dissertation. Thank you to Neil Kennedy for the initial contributions to this report, as well as for the dissertation topic.

I thank my family, especially my parents, Jill and Steve Gorven for their endless love and support. I would not have survived my university career without it. More thanks goes to the 2017 M.Phil class for making this tough degree an enjoyable and fulfilling experience.

Lastly, thank you to BANKSETA for the funding they provided for this year of study.

Contents

List of Figures

List of Tables

Chapter 1

Introduction

1.1 Research Overview

Choosing a model is of central importance in mathematical finance. The chosen model may be used for anything from pricing unlisted derivatives, to hedging calculations and risk measurement. Therefore, it is essential that the model is as tractable and plausible as possible. Geometric Brownian Motion (GBM) is a commonly used model, which leads to the seminal Black-Scholes option pricing formula (Black and Scholes, 1973). However, the Black-Scholes formula is inconsistent with certain stylised facts found in traded price data (Cont *et al.*, 2004), such as the implied volatility smile.

Stochastic volatility jump diffusion (SVJD) models account for the disparity between GBM and observation by relaxing the assumption of constant volatility and adding a jump to the security price process. The Heston model (Heston, 1993) proposes including a mean reverting stochastic volatility. The Merton model (Merton, 1976) includes lognormally distributed jumps in the security price. Finally, a model proposed by Bates (1996) combines the Heston stochastic volatility with lognormally distributed Merton jumps, creating an SVJD model.

There have been several empirical tests of SVJD models in developed markets, including work by Bakshi *et al.* (1997), Bates (2003), Chernov *et al.* (2003), and Andersen *et al.* (2002). These studies concur on the necessity of including stochastic volatility in pricing models. It appears that including jumps is also required, since just including stochastic volatility cannot describe the short maturity implied volatility smile without making the model parameters unrealistic. However, there is little information concerning the suitability of SVJD models for emerging markets. Demirgüç-Kunt and Levine (1996) and Bekaert and Harvey (1997) describe certain stylised facts associated with emerging markets such as high volatility and

low liquidity. These features may question the appropriateness of SVJD models in these markets.

Research into the suitability of SVJD models for hedging long dated financial instruments is limited, despite the common use of these models for this purpose. The volatility process used in the Heston model is mean reverting, implying that the Black-Scholes model may work equally well for long term options since the stochastic element may "wash out" to the long run mean (Heston, 1993). Additionally, the Merton model has an inverse relationship between option maturity and the skewness of the implied volatility surface. This again argues that the Black-Scholes model could perform comparably as well when used for hedging. Unanswered questions are thus raised about the benefits of this approach.

1.2 Research Aims

This dissertation aims to build an appreciation of Bates dynamics, by reducing the model to its base components: the Heston and Merton models. Furthermore, it aims to create an understanding of the effects of the Bates model parameters on pricing and hedging of vanilla options. It elucidates the challenges associated with the application of the Bates model, through an investigation into relevant estimation, calibration and simulation methods.

Since the Johannesburg Stock Exchange (JSE) represents some combination of a developed and emerging market, it is not clear how the Bates model would perform in a South African context. Therefore, this dissertation aims to assess the recovery of implied volatility surfaces from the JSE Top 40 Equity Index.

Lastly, it aims to assess the hedging capabilities of the Bates model, with an emphasis on hedging long term options. In order to reduce uncertainty surrounding the source of hedging error, a real-world environment is simulated in order to test hedging capabilities.

1.3 Notation and General Assumptions

The notation in Table 1.1 is used throughout, with further notation being defined as needed.

Notation	Description
S_t	Security spot price at t
v_t	Spot variance at t
μ	Real world drift
r	Continuously compounded risk free rate
d	Continuously compounded dividend rate
$\overline{v}$	Average long term variance
σ	Volatility of variance
κ	Mean reversion rate
μ_j	Mean log-jump
σ_j	Standard deviation of log-jump
λ	Jump intensity
Φ_t	Set of model parameters
k	Expected magnitude of jump
Z_t^i	Brownian motion i at t
K	Option strike
T	Option maturity
Moneyness	$\ln\left(\frac{K}{S_t e^{(r-d)(T-t)}}\right)$ [1]

Tab. 1.1: Notation

All models considered make the assumptions that:

- Markets are frictionless (no transaction costs, taxes, continuous trading, no short selling restrictions)
- The risk free and dividend rates are known and constant

[1] This representation of moneyness was chosen to preserve the downward sloping implied volatility surface, while also accounting for risk-neutral drift in stock price

Chapter 2

The Bates Model and its Components

2.1 The Heston Model

Heston (1993) proposes a model that accounts for the observed stochastic volatility present in markets. Unlike previous stochastic volatility models, the Heston model has a semi-closed form solution for several types of derivatives, including European vanilla options. The Heston price process is given by equation (2.1).

$$\frac{\mathrm{d}S_t}{S_t} = \mu dt + \sqrt{v_t}\mathrm{d}Z_t^1 \tag{2.1}$$

An Ornstein-Uhlenbeck process is used to describe stochastic volatility. An application of Ito's lemma then results in a mean reverting stochastic variance of the form given by equation (2.2). Gatheral (2011) notes several observed trends which are consistent with Heston volatility. The mean reversion characteristic of this equation is consistent with observed mean reverting variance. The change in variance is also linked to its current level which is consistent with the observed heteroscedasticity in variance. This process also induces variance clustering, as is commonly observed in the market.

$$\mathrm{d}v_t = \kappa(\overline{v} - v_t)\mathrm{d}t + \sigma\sqrt{v_t}\mathrm{d}Z_t^2 \tag{2.2}$$

The Brownian motions in these two SDEs are correlated as per equation (2.3). This allows the Heston model to reflect the so-called leverage effect: movements in volatility are invariably negatively correlated with movements in security price.

$$\langle \mathrm{d}Z_t^1, \mathrm{d}Z_t^2 \rangle = \rho \mathrm{d}t \tag{2.3}$$

If equation (2.4) holds, then the Feller property is satisfied, ensuring that the variance process will be strictly positive (Kienitz and Wetterau, 2012). This adds plausibility to the model.

$$2\kappa\overline{v} \geq \sigma^2 \tag{2.4}$$

For a risk-neutral implementation of this model, μ is replaced with $r-d$ in equation (2.1).

Vanilla European options can be priced using the closed form characteristic function of this model given in equation (A.5), in conjunction with quadrature of the Gil-Pelaez option pricing formula given in equation (A.4). Although this method of option pricing manages to match long term volatility surfaces, it fails to create a short term skew that corresponds with what is observed in the market under reasonable dynamics.

2.2 The Merton Model

Merton (1976) proposes a model that incorporates discontinuous jumps in the security price process. The jump size is random and is assumed to be lognormally distributed. This results in the following price process

$$\frac{\mathrm{d}S_t}{S_t} = \mu \mathrm{d}t + \sqrt{\overline{v}}\mathrm{d}Z_t + (y_t - 1)\mathrm{d}q_t \tag{2.5}$$

Here, $\mathrm{d}q_t$ is a Poisson process:

$$\mathrm{d}q_t = \begin{cases} 0 \text{ with probability } 1 - \lambda\ \mathrm{d}t \\ 1 \text{ with probability } \lambda\ \mathrm{d}t \end{cases} \tag{2.6}$$

The random drivers of these processes are assumed to be uncorrelated. This results in jumps that are uncorrelated with the market. In other words, the behaviour of stock price does not affect the probability or size of the jumps. Mathematically, this can be written as:

$$\langle \mathrm{d}Z_t, \mathrm{d}q_t \rangle = 0$$

The assumption of log-normal jumps implies that the random variable y_t is distributed as

$$\ln(y_t) \sim \mathcal{N}(\mu_j, \sigma_j)$$

The expected magnitude of these jumps is given by $k = \mathbb{E}[y_t - 1] = e^{\mu_j + \frac{\sigma_j^2}{2}} - 1$, which implies a jump variance of $\mathbb{V}[y_t - 1] = e^{2\mu_j + \sigma_j^2}(e^{\sigma_j^2} - 1)$. If the drift is chosen to be $r - d - \lambda k$, then the discounted security price is a risk-neutral martingale.

Vanilla European options written on a security with these dynamics can again be priced using the Gil-Pelaez formula in conjunction with the closed form characteristic function given in equation (A.6). Merton option prices account for the volatility skew of short dated options. This is as a result of a large jump being able to noticeably change an options value, even when the option is close to maturity. However, the stochastic volatility observed in markets remains unaccounted for, and the fit to a volatility surface with longer maturities is often unsatisfactory.

2.3 The Bates Model

Bates (1996) proposes a model that incorporates both stochastic volatility and jumps, in essence combining the Merton and Heston models. The Bates model has a price process of the following form

$$\frac{\mathrm{d}S_t}{S_t} = \mu \mathrm{d}t + \sqrt{v_t}\mathrm{d}Z_t^1 + (y_t - 1)\,\mathrm{d}q_t \tag{2.7}$$

Here, the dynamics of v_t is given by equation (2.2) (with the correlation between the Brownian motions given by equation (2.3)). The risk-neutral implementation of this model involves replacing μ with $r - d - \lambda k$.

Vanilla European options following Bates dynamics can be priced using the Gil-Pelaez formula in conjunction with the closed form characteristic function given by equation (A.7).

The Bates model gains additional value by producing a better fit for both short and long maturity implied volatility surfaces. In addition, it accounts for both stochastic volatility and jumps in security prices. This produces more reasonable parameters, as both jumps and stochastic volatility contribute to the implied volatility smile. However, there are still areas that conflict with empirical observations. For example, the model assumes that a jump in security price will have no effect on the variance. Gatheral (2011) notes that a large move in the underlying is often followed by a jump in volatility, but the Bates model has these random variables uncorrelated. This model also assumes constant mean reversion and volatility of variance parameters, whereas empirical evidence would suggest that these parameters are time dependent.

Chapter 3

Bates Implied Volatility Surfaces and Deltas

A model's ability to produce realistic implied volatility surfaces is a measure of its plausibility. Therefore, the flexibility of this surface is an important factor to consider when choosing a model. Each model parameter affects the implied volatility surface differently, and consequently a review of these effects is critical to producing a variety of volatility surfaces in the Bates model framework. In the analysis that follows, the parameters are grouped in pairs that have similar effects on the surface. This choice aids in understanding the problems of calibration. Often, one parameter may accidentally dominate another parameter with a similar effect. The base scenario model parameters used to produce these surfaces can be found in Table B.1.

It is also useful to consider the delta values that various combinations of parameters give. To give context to these delta values, they will be compared to the delta calculated using the Black-Scholes model. The left panel in Figure 3.1 displays the Bates delta implied by the base scenario parameters. A Black-Scholes model is then calibrated to the option prices that the Bates model produces. The resulting Black-Scholes delta is overlaid on the Bates delta. The difference between these two surfaces is plotted in the right panel. Delta is directly linked to the amount of underlying held in a delta hedge portfolio for a vanilla option. This analogy can be used to quantify the impact of differing delta values. If the deltas differ by 0.01, this would imply one hedging portfolio will hold 1% more (in nominal terms) of the underlying than the other.

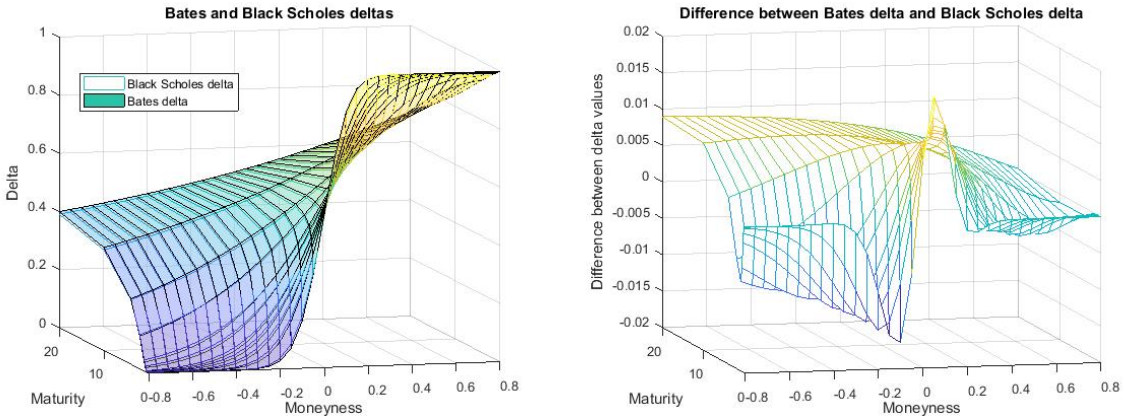

Fig. 3.1: Comparison of delta values for the Bates and Black-Scholes models

Clearly, the deltas are very similar for both models. The remaining delta comparisons in this chapter aim to find which parameters cause the Black-Scholes and Bates deltas to diverge, as these are the types of volatility surfaces where the Bates model gives significantly more information about the delta than the standard Black-Scholes model.

3.1 Correlation and Volatility of Variance

The correlation in equation (2.3) determines the relationship between movements in security price and movements in volatility. This may be used to produce the leverage effect, which requires a negative correlation value. In conjunction with the mean log-jump parameter (see section 3.4), this allows the surface to exhibit the downward sloping skew often observed in the market. The left graph in figure 3.2 exhibits this effect, with a correlation of -0.6 giving the steepest downward slope. It should be noted that a correlation of 0.6 does not give an upward sloping skew at short maturities, but rather a smile. Again, this is due to the chosen mean log-jump parameter. However, at longer maturities, the surface begins to exhibit an upward skew rather than a smile.

The volatility of variance parameter in essence scales the correlation. The larger this parameter, the more influence the correlation has on the variance process, and therefore the steeper the curve. The right graph in figure 3.2 displays this, with high values of σ resulting in a steep skew. This is in contrast to the low value of σ, which gives almost no skew at all at the long end of the surface.

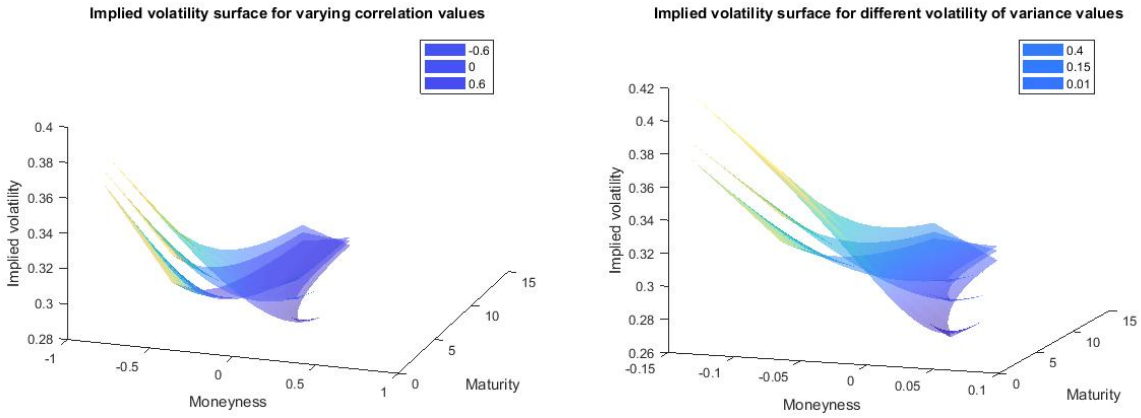

Fig. 3.2: Implied volatility surfaces for various values of ρ and σ

These two parameters can create a trade-off effect when matching the skew of the curve. The correlation value gives the curve's overall inclination, which the volatility of variance then scales. Surfaces with a skew can either be matched with a small value for ρ paired with a large σ value, or vice versa. The correlation value can lie between -1 and 1, but empirical evidence presented by Bates (2000) suggests it is often negative. The volatility of variance however must fulfil the Feller property, which restricts its magnitude relative to κ and $\overline{v}$.

Figure 3.3 displays the relationship between these parameters with respect to the delta they produce. The difference between Black-Scholes and Bates deltas is negligible at long maturities, except when both volatility of variance and the magnitude of correlation is high. This combination of parameters produces an implied volatility surface like that displayed in the bottom graph of this figure. It has a fairly consistent skew, even at longer maturities, which the Black-Scholes delta cannot account for correctly. The difference in deltas on the short end of the curve is less affected by these parameters.

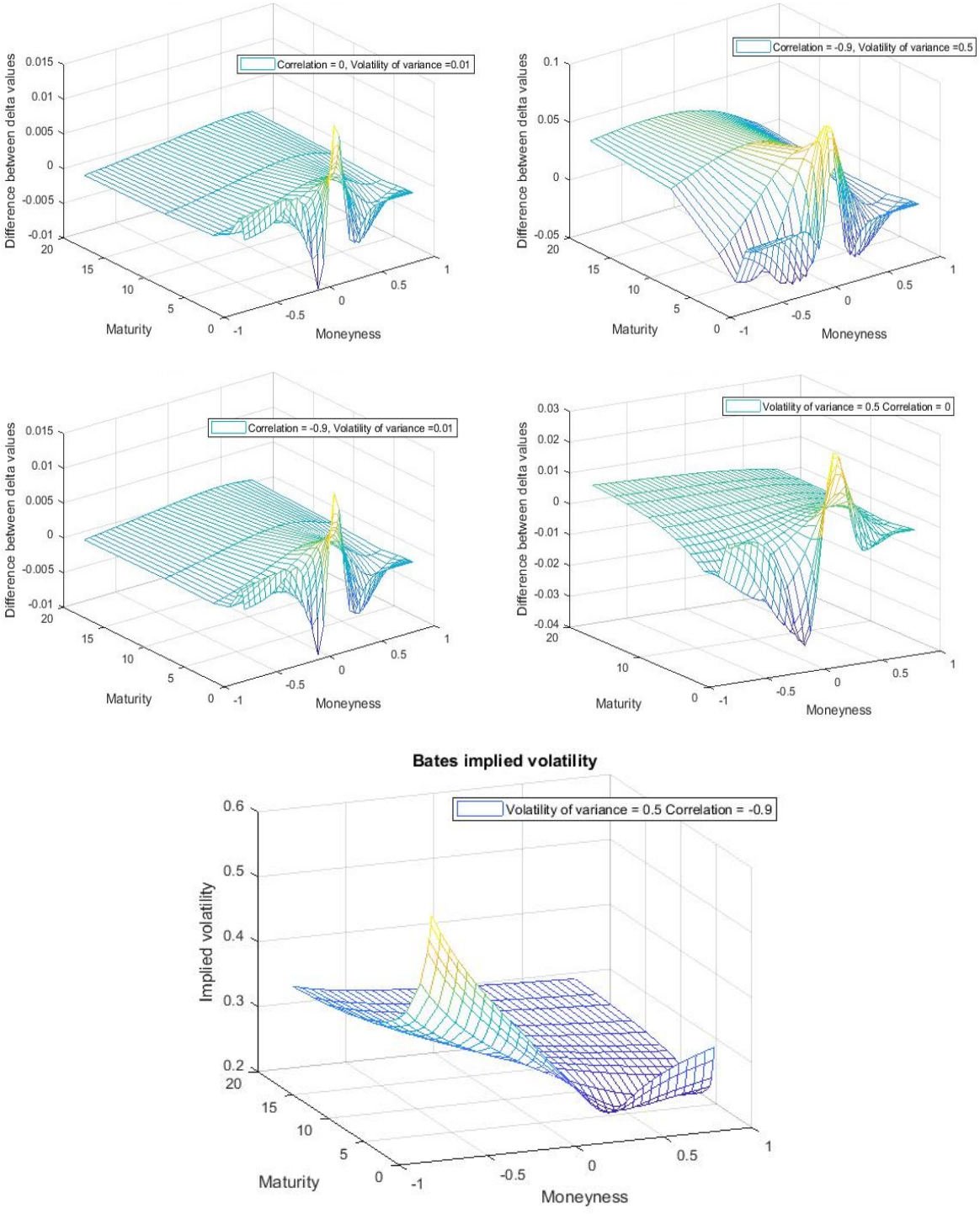

Fig. 3.3: Delta comparisons for various values of ρ and σ

3.2 Spot Variance and Long Term Variance

Although spot variance is a state process rather than a model parameter, it must be estimated, since it is hidden in the price process data series. This estimation is often combined with model calibration (see Chapter 4), and therefore a discussion of its effect on the implied volatility surface is useful. The left graph in figure 3.4, clearly shows that the height of the short end of the surface is highly dependent on the spot variance with a higher spot variance corresponding to a higher surface. The surfaces begin to converge for longer maturities, indicating that the process is expected to settle down to the long term variance. Nevertheless, it should be noted that the surfaces are always separated, implying that spot variance still has some effect on long term options.

Conversely, in the right graph, the level of the long end of the surface is highly dependent on the long term variance, and the short end less so. Again, the larger the long term variance, the higher the surface.

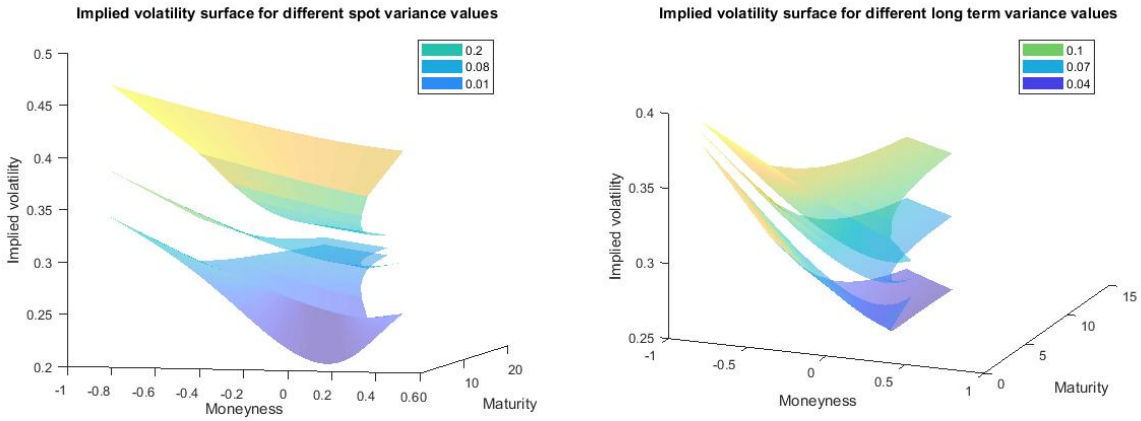

Fig. 3.4: Implied volatility surfaces for various values of v_0 and $\overline{v}$

Although v_0 and $\overline{v}$ may seem to have opposite effects, figure 3.5 conveys their similarities for a single maturity. This emphasises the importance of calibrating to a volatility surface with several spaced-apart maturities, in order to avoid confusing their effects.

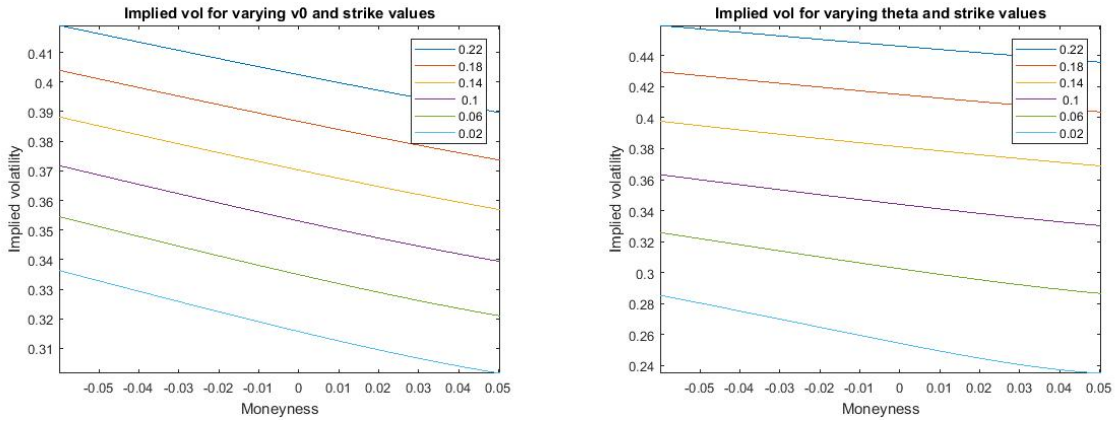

Fig. 3.5: Implied volatility curves with a maturity of 2 years for various values of v_0 and $\overline{v}$

From figure 3.6 it is evident that the Black-Scholes delta is significantly different from the Bates delta when the long term and spot variances are significantly different. This is likely because a constant Black-Scholes volatility can only be near to either the short or long term volatility. Therefore, one of the ends of the surface will be (possibly severely) misspecified. Generally, since only short term options are available for calibration, the Black-Scholes volatility will be closer to the short end volatility, and therefore the long end of the surface, and corresponding delta, will be misspecified. Consequently, surfaces of the type shown in the bottom graph of figure 3.6 should be treated with caution when using the Black-Scholes delta to hedge long term options.

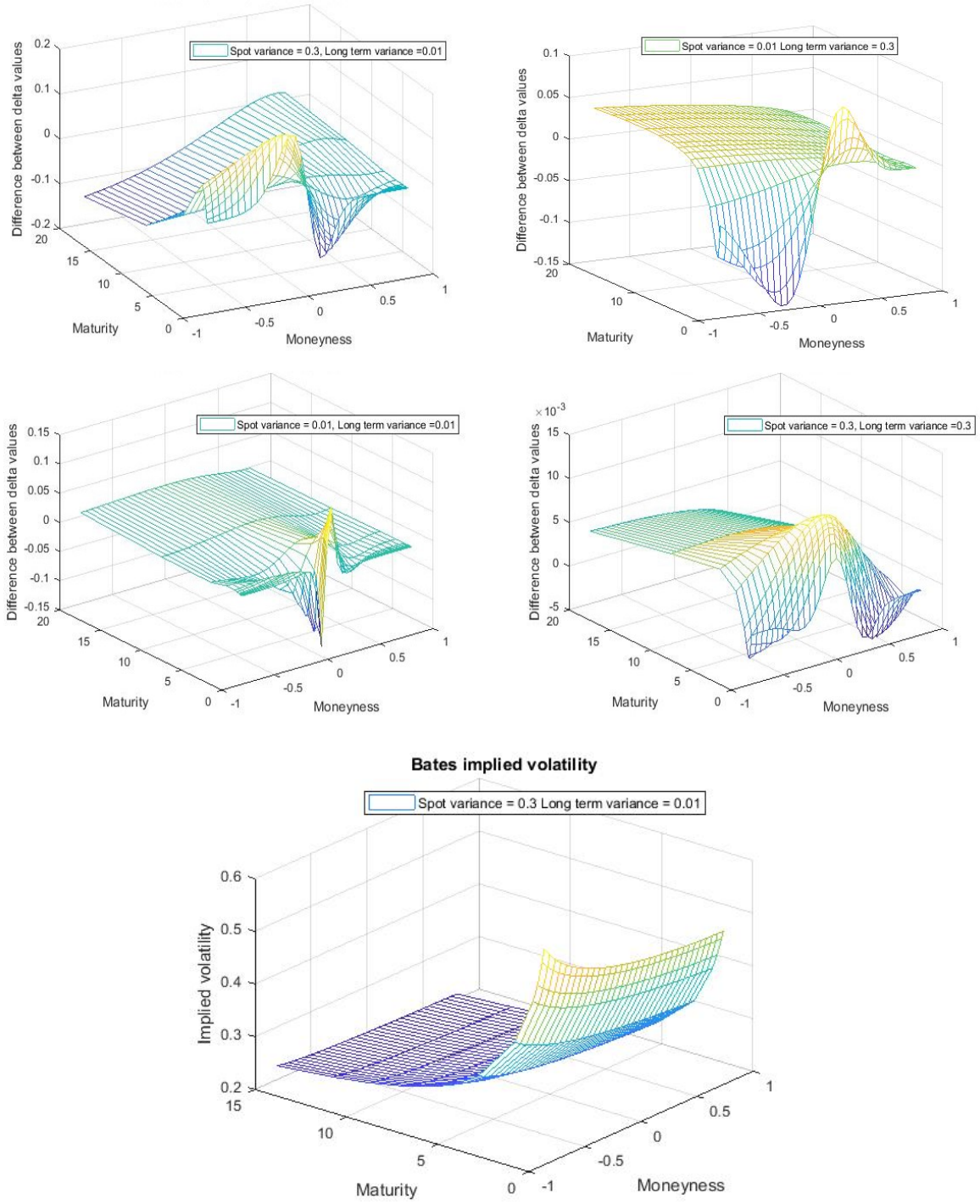

Fig. 3.6: Delta comparisons for various values of v_t and $\overline{v}$

3.3 Mean Reversion

Mean reversion of variance can be understood in a fairly intuitive style as being the speed at which the spot variance reverts to the long term variance. For this reason, the base scenario spot variance was adjusted to 0.2 (significantly different from the 0.07 long term variance) for this comparison. The left graph in figure 3.7 conveys how high values of κ result in a steep descent from the short to long end of the surface. The surface quickly levels out when the long term volatility is matched. Low κ values give the surface a more gradual descent. A second effect is the reduction of skew at the long end of the curve. If we assume that the leverage effect exists, downward movements in security prices (negative returns) will on average result in upward movements in volatility. However, if κ is large, these upward movements will quickly be cancelled out by the mean reversion. This results in a flatter long term skew.

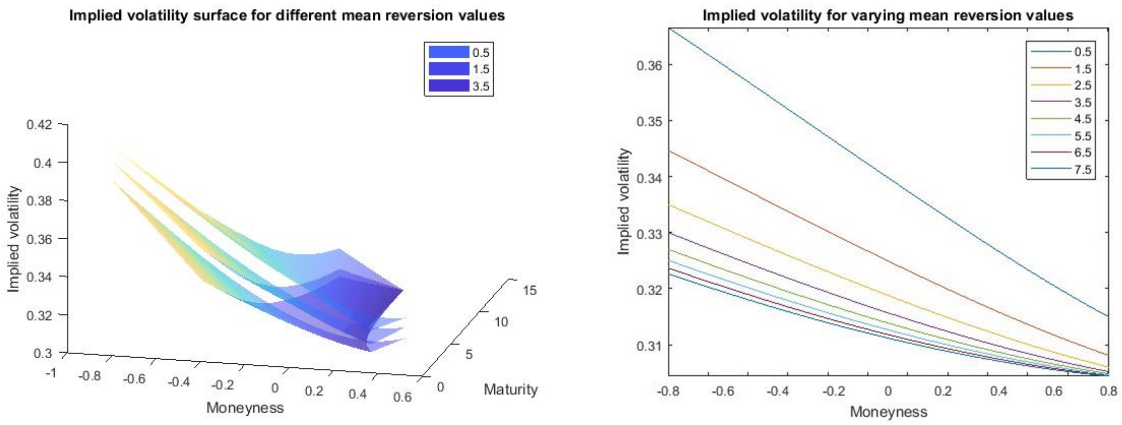

Fig. 3.7: Implied volatility surface, and implied volatility line graph at a maturity of 2 years for various values of κ

The right graph in figure 3.7 conveys how the implied volatility curve tends to a limiting curve as the mean reversion parameter increases. For this reason, the only restriction applied to this parameter is that it must be positive and obey the Feller condition. However, large values of κ are likely a result of trying to fit the short term skew of a surface through using a high σ value in conjunction with a large κ.

Figure 3.8 again displays the link between mean reversion and volatility of variance. A high volatility of variance combined with a high mean reversion results a fairly accurate Black-Scholes delta, but when volatility of variance is high and mean

reversion is low, the difference is larger. This is because high mean reversion forces the surface to its long term variance more quickly, resulting in less of a difference between the short and long end of the surface. However, when mean reversion is low, the difference between the short and long ends of the surface are more pronounced, resulting in a larger difference. The enhanced long term skew from a low mean reversion value also contributes to this effect.

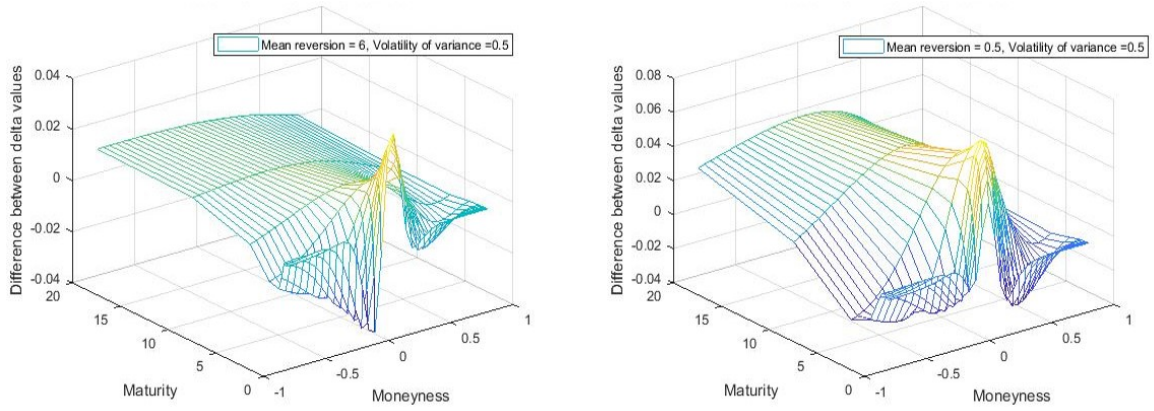

Fig. 3.8: Delta comparisons for various values of κ and σ

3.4 Jump Parameters

Mean log-jump

As implied by the name, the mean log-jump indicates where the jump is centred. If the log-jump is centred around a highly negative value, then the resulting jumps will range from large and negative to small and positive. Consequently, the downward skew is the most emphasised for a mean log-jump of -0.2, as demonstrated in the right panel of figure 3.9. Conversely, if the average log-jump is positive, the resulting jumps will range from large and positive to small and negative. The surface with the highest front right tip in the same panel therefore corresponds to a mean log-jump of 0.1. Finally, if the jump is centred close to 0, both in and out the money options should be affected equally, resulting in a smile effect. However, these jumps will have smaller magnitude, because neither side is emphasised. This results in a slightly lower implied volatility surface. This is displayed by the lowest surface in the panel, which corresponds to a mean log-jump of -0.05. This figure also demonstrates how the skew of the long end of the curve is relatively unaffected by the choice of mean log-jump.

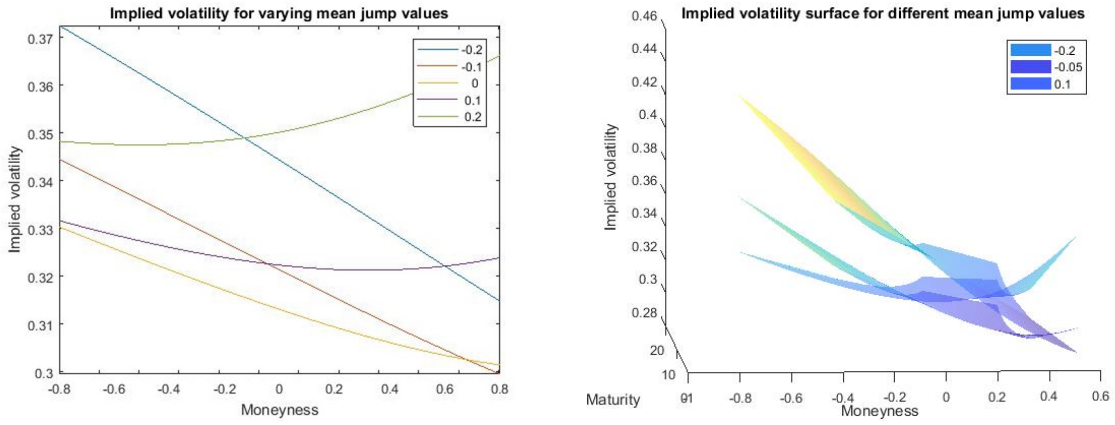

Fig. 3.9: Implied volatility line graph at a maturity of 2 years, and implied volatility surface for various values of μ_j

The expected mean log-jump is often negative. This is because markets traditionally crash more than they boom. In addition, a negative mean log-jump adds to the downward sloping skew often observed in markets (Bakshi *et al.*, 1997).

Jump intensity and deviation

Jump intensity determines how frequently jumps occur. A large jump intensity has the effect of increasing the volatility of the underlying, which results in a higher implied volatility surface, which can be seen clearly in the left graph in figure 3.10.

The standard deviation of the log-jump determines how far away from k the jumps can stray. A jump-deviation of 0 would imply that jumps are always the same size. A high jump deviation therefore creates the possibility for jumps much larger than k, which is generally close to 0. Large jumps increase the volatility of the underlying, and therefore having a high corresponding implied volatility surface. However, this parameter has the added effect of making options that are deep in or out of the money more valuable, due to the possibility of their value changing significantly, as is clear in the right graph. This results in a exaggerated smile for short term options, and implies that having options with a wide range of strikes to calibrate to is important, as otherwise jump intensity and deviation of jump have very similar effects.

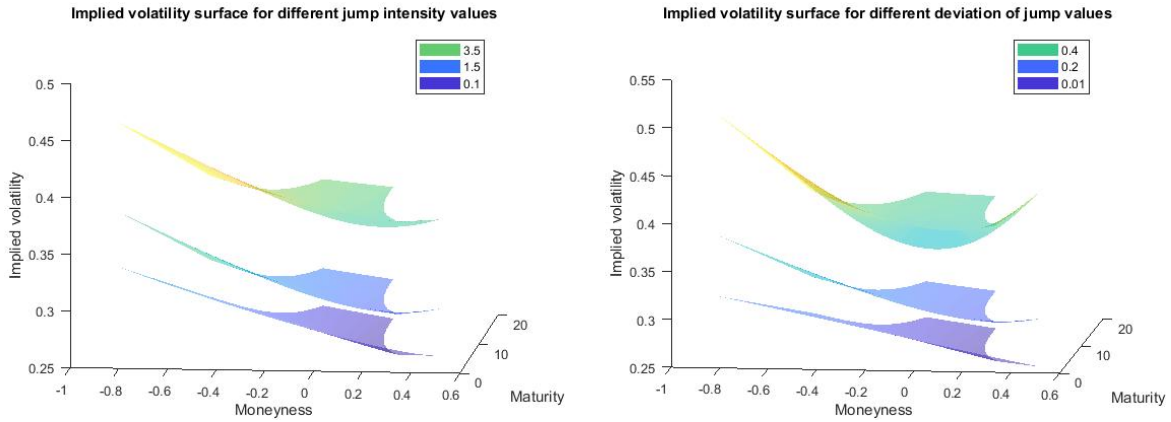

Fig. 3.10: Implied volatility surfaces for various values of λ and σ_j

Jump components and deltas

The jump components mainly affect the short end of the delta surfaces. The top right graph in figure 3.11 illustrates how no jump component causes the short maturity Bates delta to be similar to the Black-Scholes delta. Conversely, a large jump intensity and deviation causes the short term deltas to be quite different. The mean log-jump value dictates whether the short term delta is over or under estimated, as is clear from the bottom two graphs. No matter which jump parameters are chosen, the long end of the surface is fairly similar to the Black-Scholes equivalent, again emphasising that jumps have more of an effect on short term options.

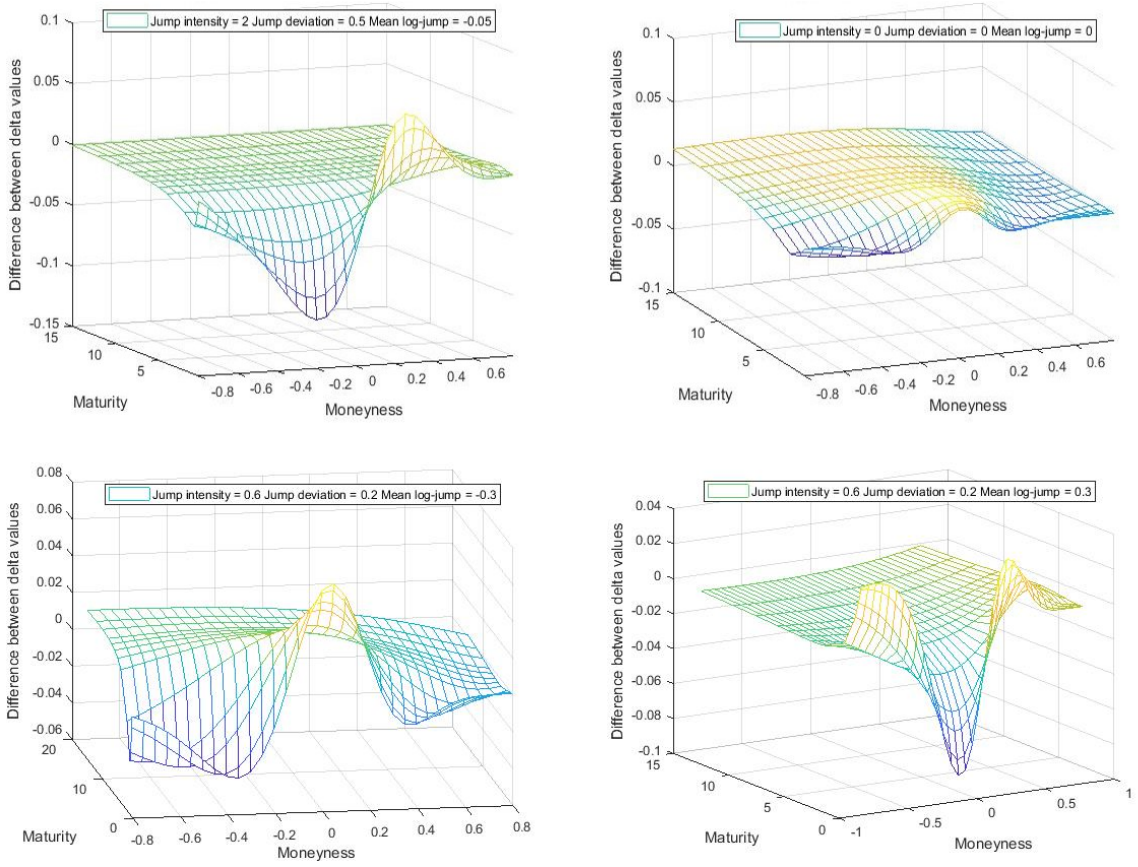

Fig. 3.11: Delta comparison for various jump parameters

Chapter 4

Estimation, Calibration and Simulation

4.1 Risk-Neutral Parameter Calibration and Variance Estimation

A risk-neutral calibration of model parameters and spot variance, through the minimisation of a loss function, is presented below. This approach is adapted from Bakshi *et al.* (1997). Risk-neutral calibration is chosen for two main reasons. Firstly, it negates the need to estimate risk-premia when pricing securities, as these have already been incorporated into the observed price of the security in question. Secondly, when using options for risk-neutral calibration, the data has a forward outlook. In other words, these prices depend on the market's expectation of the future, rather than depending on past realisations in a time-series calibration approach. An additional benefit is the relevancy to industry, as risk-neutral calibration is used almost exclusively for pricing and hedging.

4.1.1 Calibrating to Option Prices

The objective for calibrating a model to option prices is clearly to have the model reproduce the option prices as closely as possible. Consequently, the first logical step is to attempt to minimise the distance between observed option prices in the market and model option prices. The parameters that minimise this distance are referred to as optimal model parameters. The Residual Mean Squared Error (RMSE) between observed option prices and model produced option prices can be expressed as a function of model parameters and spot variance, as given by equation (4.1). This gives some notion of distance between observed and model prices, with a large

RMSE implying a large distance between prices.

$$RMSE_X(v_t, \Phi_t) = \frac{1}{N}\sum_{n=1}^{N}\left(\widehat{X_n}(t, T_n, K_n) - X_n(t, T_n, K_n; v_t, \Phi_t)\right)^2 \tag{4.1}$$

Here, the n^{th} observed option price is represented by $\widehat{X_n}(t, T_n, K_n)$. As the notation implies, option prices are unique for different strikes, maturities and times [1]. Model option prices are denoted by $X_n(t, T_n, K_n; v_t, \Phi_t)$.

For SVJD models, option prices are a function of security spot price, option strike, option maturity, current time, spot variance and model parameters. As the spot variance is a hidden process, it must be estimated along with the model parameters. All other variables will correspond to the n^{th} observed option. Therefore, the model can be calibrated via the optimisation problem in equation (4.2).

$$[v_t^{opt}, \Phi_t^{opt}] = \underset{v_t, \Phi_t}{\arg\min}\left(RMSE_X(v_t, \Phi_t)\right) \tag{4.2}$$

It must be noted that the spot variance v_t is unique for each t. Therefore, the optimisation scheme must be applied to options at a single point in time, even though model parameters are assumed to be stationary.

Bakshi *et al.* (1997) notes that, as this loss function measures the magnitude of the difference between prices, it can be criticised for putting less emphasis on out the money options, due to this type of option having low prices to begin with. A percentage difference is often suggested in the literature to correct this flaw. However, Bakshi *et al.* (1997) argues that the percentage difference approach has the opposite problem of weighting in the money options less than out the money options.

4.1.2 Calibrating to Implied Volatilities

A second plausible loss function considered is the RMSE between observed and model produced implied volatilities. The loss function and corresponding optimisation problem are given in equations (4.3) and (4.4) respectively.

$$RMSE_{IV}(v_t, \Phi_t) = \frac{1}{N}\sum_{n=1}^{N}\left(\widehat{IV_n}(t, T_n, K_n) - IV_n(t, T_n, K_n; v_t, \Phi_t)\right)^2 \text{ [2]} \tag{4.3}$$

[1] Option prices are also a function of spot price, risk-free interest rate and dividend rate. However, the spot price is considered to be encompassed by the current time. The risk-free interest rate and dividend rate are constant and known, and are therefore not mentioned.

[2] $RMSE_{IV}$ values shown in tables are multiplied by 100 for ease of reading.

$$[v_t^{opt}, \Phi_t^{opt}] = \underset{v_t, \Phi_t}{\arg\min} \left(RMSE_{IV}(v_t, \Phi_t) \right) \tag{4.4}$$

Observed implied volatilities are denoted by $\widehat{IV_n}(t, T_n, K_n)$, whereas model implied volatilities are given by $IV_n(t, T_n, K_n; v_t, \Phi_t)$. Implied volatilities have the same dependencies as their option counterparts, but do not put the same emphasis on in the money options. Although implied volatilities are generally higher for out the money options, the difference in magnitude is far less in comparison to the difference in magnitude between option prices. However, this loss function requires an additional step of converting model option prices to implied volatilities inside the optimisation procedure, which may introduce complications. Both loss functions will therefore be considered.

4.1.3 Adding a Penalty Term

As the Bates model has several parameters, some of which have linked effects, calibration can often result in switching emphasis between linked parameters. This leads to highly volatile parameters, as well as neglect of the unemphasised parameter. A possible approach to dealing with this issue is adding a penalty term to the loss function as expressed in equation (4.5).

$$[v_t^{opt}, \Phi_t^{opt}] = \underset{v_t, \Phi_t}{\arg\min} \left(RMSE(v_t, \Phi_t) + \eta \cdot |\Phi_{t-1}^{opt} - \Phi_t| \right) \tag{4.5}$$

Here, η is a vector that chooses how to scale the penalty associated with each parameter in this function. The i$^{\text{th}}$ value of η corresponds to the i$^{\text{th}}$ parameter in Φ_t. If $\eta(i)$ is large, then movement in the i$^{\text{th}}$ parameter will be highly discouraged, as movement in this parameter will add a significant amount to the minimisation problem. Therefore, the choice of η is important, as this determines how constricted each parameter is. If the value of η is too large, the calibration will not be able to function properly, as the parameters will be unable to move. On the other hand, if η is too small, this term will have a negligible effect on calibration.

4.1.4 Minimisation of Loss Function

All the calibration schemes considered here involve minimisation of a loss function. The built in MATLAB implementation of the SQP algorithm was used in all cases. This algorithm is recommended by Kienitz and Wetterau (2012) for its speed, global convergence and ability to implement non-linear restrictions, such as the Feller condition. The global version of this algorithm can be implemented through the use of fmincon in conjunction with the GlobalSearch toolbox. However, due to time

constraints, as well as minimal improvements in parameters, the local version was employed for calibration to simulated data.

4.2 Bates Simulation

Accurate simulation of the state processes of a model has several applications, among which is the Monte Carlo approach for pricing exotic instruments with no closed form solution. Simulation of a SVJD type model involves discretisation of the continuous state variables, and therefore becomes an approximation rather than an exact representation of the process. Another common issue in simulation of the Bates model is ensuring non-negative variance. Gatheral (2011) notes that satisfying the Feller condition is no longer sufficient to ensure an always positive variance, and therefore a reflective or absorbing condition is required. Furthermore, traditional schemes such as the Milstein discretisation do not account for jump-type processes, and therefore, a different sampling method is needed.

4.2.1 Algorithm

Cont *et al.* (2004) present a method of simulating jump-diffusion processes using fixed grid sampling for the independent jump component, leaving the simulation of the rest of the process free to follow traditional methods. This framework is followed here, using a Milstein approximation for the rest of the process. Negative variance is prevented by taking the maximum of the discretised variance process and 0. This is not technically an absorption condition, as the mean reversion causes the variance to drift towards the long term variance, even if the current value of variance is 0. The simulation of the log security process, conditional on knowing the initial price (S_0) and variance (v_0), is described below:

Step 1: For the chosen sampling frequency dt, calculate the number of periods required: $N_m = \frac{T}{dt}$

For: $i = 1 : N_m$ do Steps 2-5

Step 2: Sample a random variable $N_k \sim P(\lambda dt)$, representing number of jumps realised in the period.

Step 3: Sample three standard normal random variables Z_t^1, Z_t^2 and Z_t^j. Let $Z_t^s = Z_t^1$ and $Z_t^v = \rho Z_t^1 + \sqrt{1-\rho^2} Z_t^2$

Step 4: $\ln(S_i) = \ln(S_{i-1}) + (r - d - \frac{1}{2}v_{i-1} + \lambda k)dt + \sqrt{v_{i-1}dt} Z_t^s + N_k \mu_j + \sqrt{N_k}\sigma_j Z_t^j$

Step 5: $v_i = \max\left[(\sqrt{v_{i-1}} + \frac{1}{2}\sigma\sqrt{dt} Z_t^v)^2 + \kappa(\overline{v} - v_{i-1})dt - \frac{1}{4}\sigma^2 dt \quad ; \quad 0\right]$

A comparison of vanilla call prices using a Monte Carlo calculation, to prices using the Gil-Pelaez formula, can be found in section B.2.

4.2.2 Parameter Effect on Simulation

A brief summary of parameter effects on simulation is useful for a deeper understanding of the model. Furthermore, it demonstrates empirical effects often observed in the market.

Security Price and Volatility

The relationship between a securities price and its variance is largely based on the correlation and mean reversion values chosen.

The leftmost graph in Figure 4.1 depicts a Bates simulation using a correlation value of -0.9. Here the leverage effect is clear, as downward movements in security price are almost always followed by an upward jump in variance, resulting in high variance for low stock prices and vice versa. A low mean reversion parameter is used to emphasis this effect. In the rightmost graph a higher mean reversion parameter makes the mean reversion effect clearer. Downward jumps in security price still result in upward jumps in variance, but instead of staying high, the mean reversion effect quickly pushes it back to the chosen long term variance of 0.07.

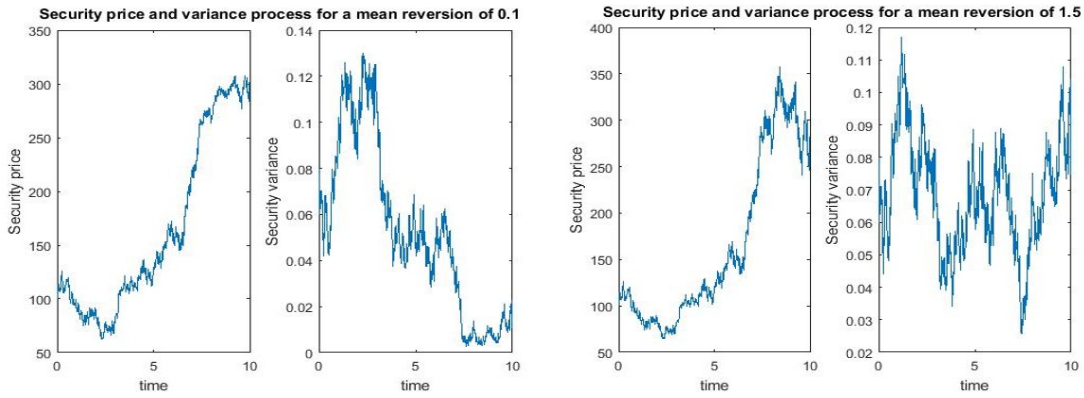

Fig. 4.1: Simulated security price and variance for different mean reversion values

Returns

The effect of the jump component is best demonstrated with security returns. The left graph in Figure 4.2 displays daily returns with jumps. Abnormal returns are clearly visible, with several days having returns far beyond what would "normally" be expected. Conversely, the right graph has returns constrained below 0.1 and above -0.1. It should be noted that the jumps also have the effect of increasing the apparent volatility of the security.

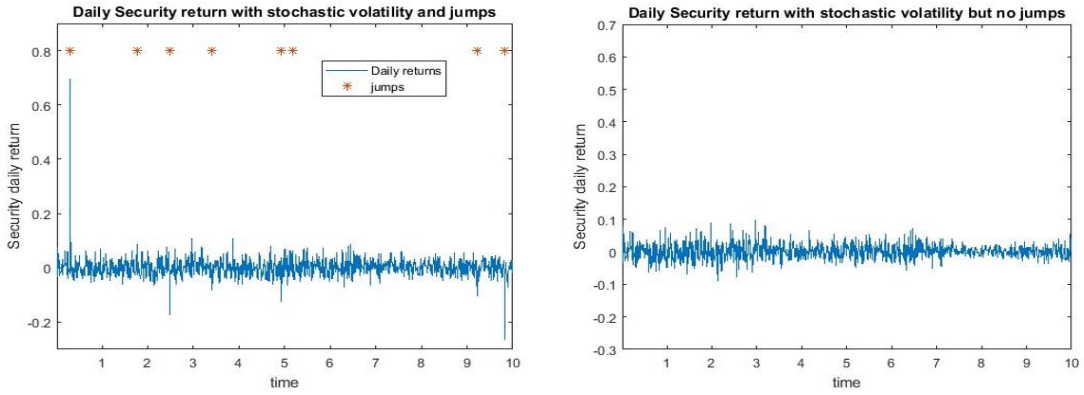

Fig. 4.2: Daily security returns with and without jumps

The volatility clustering effect is also evident in returns. Figure 4.3 exhibits this clustering, as well as showing that the location of clustering is dependent on the correlation value used. A low mean reversion parameter is used here to emphasise this effect.

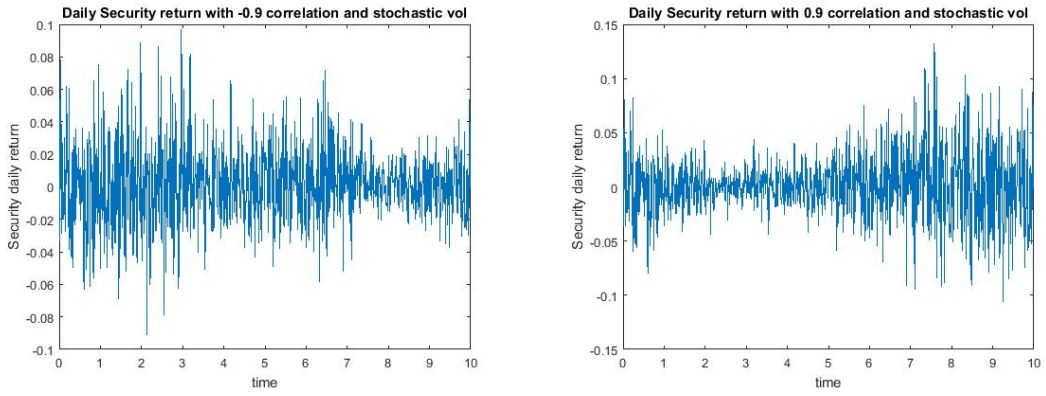

Fig. 4.3: Daily security returns without jumps for different correlation values

Chapter 5

Hedging

To compare the hedging performance of the Bates model to industry standards, the Black-Scholes and local volatility (LV) models are implemented. To separate and assess the effects of stochastic volatility and jumps on hedging, the Heston and Merton models are also considered. The dynamics of LV model can be found in section A.3.1.

5.1 Hedge Strategy

For simplicity and comparability, a delta hedge strategy is chosen, following the approach of Bakshi *et al.* (1997). Assuming Bates dynamics, it is clear that there are two sources of stochastic variation which affect option value. These are security price and variance. The sensitivities of option value to these variables are described by equations (5.1) and (5.2), respectively. Therefore, both a variance sensitive instrument and a security price sensitive instrument must be held for a full hedge under Bates dynamics. It should be noted that, in a Bates setting, the jumps in security price imply an incomplete market, and a perfectly replicating hedge portfolio is not possible even assuming continuous rebalancing. This jump risk is considered unhedgeable, and therefore is not considered further. The hedge portfolios constructed in this section aim to have the same sensitivities to state variables as the hedged option. These portfolios are then shorted to hedge the option in question.

$$\Delta_s(t;T,K) = \frac{\partial X(t;T,K)}{\partial S} = e^{-d(T-t)}Q_1 \tag{5.1}$$

$$\Delta_v(t;T,K) = \frac{\partial X(t;T,K)}{\partial v} = S_t e^{-d(T-t)}\frac{\partial Q_1}{\partial v} - Ke^{-r(T-t)}\frac{\partial Q_0}{\partial v} \tag{5.2}$$

Q_1 and Q_0 in equations (5.1) and (5.2) reference the Gil-Pelaez probabilities in equation (A.3). The partial derivatives with respect to variance of these probabilities are calculated using finite differences. Equation (5.2) represents the sensitivity

of the option to variance, which must be hedged by a shorting a different variance sensitive instrument with an equal sensitivity. However, for two reasons, a holding in a variance sensitive instrument is problematic:

1. Comparability of models - A constant or local volatility model does not require a holding in a volatility sensitive instrument for a complete hedge, because it assumes dynamics where the variance of the underlying is constant. Therefore, it is likely that the stochastic volatility models will outperform these models because of the diversifying effect of a variance sensitive instrument (such as a vanilla option with a different strike). Therefore, for a more accurate comparison, a Black-Scholes vega hedge must be used in addition to a delta hedge for constant and local volatility models.

2. Long term hedging - Long term hedging using options is both expensive and challenging. It is not reasonable to assume that long term options can be liquidly traded, especially in the context of the JSE. Consequently, the options held for hedging purposes must be of shorter maturity than the hedged instrument. This introduces complications, as the instrument used for hedging must be sold and bought several times during the life of the hedge.

Accordingly, one of the hedge portfolios considered consists of a holding in the underlying (β_s) and in the money market account (A_t).

$$\beta_s(t_i) = \Delta_s(t_i; T, K) \tag{5.3}$$

The value of this hedge portfolio is given in equation (5.4).

$$\begin{aligned} &\Pi(t_i) = \beta_s(t_i) S_{t_i} + A_{t_i} \\ &\text{with} \\ &A_{t_0} = X(t_0; T, K) - \beta_s(t_i) S_{t_0} \end{aligned} \tag{5.4}$$

The money market account will be used to finance daily portfolio rebalancing as per equation (5.5).

$$A_{t_i} = A_{t_{i-1}} e^{r(t_i - t_{i-1})} + \left[\beta_s(t_{i-1}) - \beta_s(t_i)\right] S_{t_i} \tag{5.5}$$

A second possible hedging portfolio with holdings in a liquid vanilla option is considered. The holding in the option is denoted by β_v and the option value by X_h. This option will have a different strike ($\overline{K}$) and maturity ($\overline{T}$). The required holding for a variance hedge is given by equation (5.6).

$$\beta_v(t_i) = \frac{\Delta_v(t_i; T, K)}{\Delta_v(t_i; \overline{T}, \overline{K})} \tag{5.6}$$

The remaining sensitivity to the underlying can be hedged with a holding in the underlying:

$$\beta_s(t_i) = \Delta_s(t_i; T, K) - \beta_v(t_i)\Delta_s(t_i; \overline{T}, \overline{K}) \tag{5.7}$$

Then, the value of the hedging portfolio is:

$$\begin{aligned} &\Pi(t_i) = \beta_s(t_i)S_{t_i} + \beta_v(t_i)X_h(t_i; \overline{T}, \overline{K}) + A_{t_i} \\ &\text{with} \\ &A_{t_0} = X(t_0; T, K) - \beta_s(t_0)S_{t_0} - \beta_v(t_0)X_h(t_0; \overline{T}, \overline{K}) \end{aligned} \tag{5.8}$$

The portfolio is rebalanced daily, using the money market account as per equation (5.9). Although it may not be necessary to rebalance daily due to the holding in the option, daily rebalancing is assumed.

$$A_{t_i} = A_{t_{i-1}}e^{r(t_i - t_{i-1})} + \left[\beta_s(t_{i-1}) - \beta_s(t_i)\right]S_{t_i} + \left[\beta_v(t_{i-1}) - \beta_v(t_i)\right]X_h(t_i; \overline{T}, \overline{K}) \tag{5.9}$$

Hedge error (HE) for either portfolio is defined by:

$$HE_{t_i} = X(t_i; T, K) - \Pi(t_i) \tag{5.10}$$

Hedging error has a cumulative effect due to the interest earned or paid on the money market account. This, along with path dependency, makes hedge error hard to interpret. Therefore, absolute average hedging error (AAE) is considered. First, the value of a static hedging portfolio created at time t_c can be described for the two hedging portfolios by equations (5.11) and (5.12), respectively.

$$\Pi_{t_c}(t_i) = A_{t_c}e^{r(t_i - t_c)} + \beta_s(t_c)S_{t_i} \tag{5.11}$$

$$\Pi_{t_c}(t_i) = A_{t_c}e^{r(t_i - t_c)} + \beta_s(t_c)S_{t_i} + \beta_v(t_c)X_h(t_i, \overline{T}, \overline{K}) \tag{5.12}$$

The initial value of the money market account (A_{t_c}) is given by the respective initial conditions in equations (5.4) and (5.8). AAE can then be calculated by:

$$AAE(T, \hat{K}) = \frac{1}{N}\sum_{i=1}^{N}\left(\left|X(t_i; T, \hat{K}) - \Pi_{t_{i-1}}(t_i)\right|\right) \tag{5.13}$$

This is essentially creating a hedging portfolio at t_0 to hedge $X(t_0; T, \hat{K})$ and then measuring the absolute hedging error at t_1. A new hedging portfolio is constructed at t_1 to hedge $X(t_1; T, \hat{K})$ and the absolute hedging error is measured at t_2. This continues until t_N. The average of these absolute hedging errors is then called the AAE. In order to make this measure consistent through time, the strike

of the hedged option ($\hat{K}$) is chosen such that the moneyness of the option is always the same. This measure is less path dependent compared to hedging error. In addition, AAE is a measure of magnitude of the hedge error, which should be as small as possible, and consequently gives a clear measure of hedging performance. However, it gives no indication of whether the hedge portfolio usually over or under performs compared to the hedged instrument, as it is a measure of magnitude rather than direction. With this is mind, hedge bias (HB) is considered as defined in equation (5.14).

$$HB(T, \hat{K}) = \frac{1}{N} \sum_{i=1}^{N} \left(X(t_i; T, \hat{K}) - \Pi_{t_{i-1}}(t_i) \right) \tag{5.14}$$

This will indicate how the hedge portfolio performs relative to the hedged instrument. If this value is positive, the hedged instrument on average outperforms the hedge portfolio. If it is negative, the opposite is true.

However, both these measures are likely to oscillate at first, and amount of data required to reach a stable value is unknown. Therefore convergence of both measures is tested in section B.6.

5.2 Hedging Framework

Replication of an option payoff relies on the ability to continuously rebalance a self-financing hedge portfolio, as well as having complete knowledge of the dynamics of the underlying (assuming the dynamics imply a complete market). In reality however, the dynamics of the underlying are unknown, and it is impossible to trade continuously. This makes it difficult to identify whether hedge error is due to discrete trading, or incorrectly specified model dynamics. In addition, historical option data often does not contain prices of options with maturities longer than 3 years. Therefore, in addition to these two sources of uncertainty, extrapolation of implied volatility, as described and assessed in section B.3, is required to estimate the value of a long term instrument, such as an equity linked endowment. In order to eliminate the need to extrapolate implied volatilities as well as to understand the driving force behind the option prices, our hedging analysis is based on simulated data.

The data in question is simulated using a Bates model with autocorrelated stochastic parameters, following an arithmetic Brownian motion with a boundary reflection condition. In other words, the parameters change slowly over time, and are bounded between chosen values. The initial values of these parameters and spot

variance are given in table B.1. The initial spot security price is chosen to be 50000 index points. This simulation imposes the assumption that the market follows a Bates like process with varying parameters, which do not change much from day to day. If the parameters were chosen to be uniformly distributed between bounds, it would often be the case that implied volatility surfaces would change shape completely from day to day. This contradicts the more gradual changes observed in markets. The chosen simulation aims to approximate a real-world environment to increase the relevancy of hedging results. Additionally, simulating data in this manner allows the Bates model the best circumstances possible for hedging, as calibrated parameters should be fairly stable, and each implied volatility surface may be fitted exactly. The instrument type chosen to be hedged is a vanilla call, as it is linked to an endowment, see Section B.4.

Chapter 6

Results

6.1 Data

Real world data used in this dissertation consists of implied volatilities for options written on the JSE Top 40 Equity Index with a range of 13 strikes and 2 maturities. This range of implied volatilities is visible once every 3 months between the 31st December 2015 and the 29th of September 2017. This provides enough data for 8 volatility surfaces, each 3 months apart. The strikes range between 70% to 130% of the forward price, and the maturities given are for options expiring in 6 and 12 months. The 3 month gap between surfaces makes hedging analysis impossible, as a portfolio that is only rebalanced once every 3 months would lead to large and volatile hedging errors. Moreover, the limited available data could result in unsatisfactory calibration of the Bates model. These data limitations are specific to this study, with the 3 month gap being an unusual restriction. However, in practice other data limitations could be present, especially in the context of a developing market. Data requirements for satisfactory calibration are therefore investigated further in section 6.2.2.

6.2 Calibration and Estimation

This section investigates different types of calibration as well as the effect of input data on calibration. This is done by comparing calibrated parameters to the parameters used to simulate the data. This data consists of implied volatility surfaces and security prices, and is simulated using stochastic parameters in the same way as described in section 5.2. Through this method of comparison, a preferred calibration scheme is chosen. This is followed by using the chosen calibration method to fit JSE Top 40 Equity Index implied volatility surfaces, and then comparing this fit to other models.

6.2.1 Calibration Types

Penalty Term

The first calibration tool assessed is the penalty term described in section 4.1.3. In this case, the parameters are calibrated to call prices. Three penalty types are considered, namely, no penalty, a constant penalty and a weighted penalty. The constant penalty uses a one value for each element of η. Each element ($\eta(i)$) of the weighted penalty is related to the inverse of the expected range of the i$^{\text{th}}$ parameter. For example, if it is expected that κ will range between 0.5 and 3, but $\overline{v}$ will only range between 0.05 and 0.2, the penalty assigned to the $\overline{v}$ value will be higher than that assigned to the κ value. Figure 6.1 conveys how a penalty restricts the volatility of the calibrated parameters, bringing them closer to the parameters used to simulate the data. This is especially evident in the jump parameters. The constant penalty and the weighted penalty perform similarly at first, but once the parameters begin to settle, the weighted penalty performs the best. Some of the errors in calibration described in section 3 are evident in the no penalty case. An overestimation of jump intensity is almost always mirrored by an underestimation of jump deviation. There is a similar relationship between the correlation and volatility of variance parameters. An additional trend evident in the calibrated parameters is a relationship between mean log-jump, and jump intensity. The two parameters seem to be under or overestimated almost simultaneously. This is likely because a high jump intensity pushes the volatility surface up, whereas a mean log-jump that is close to zero compensates, and pushes the surface back down, and vice versa.

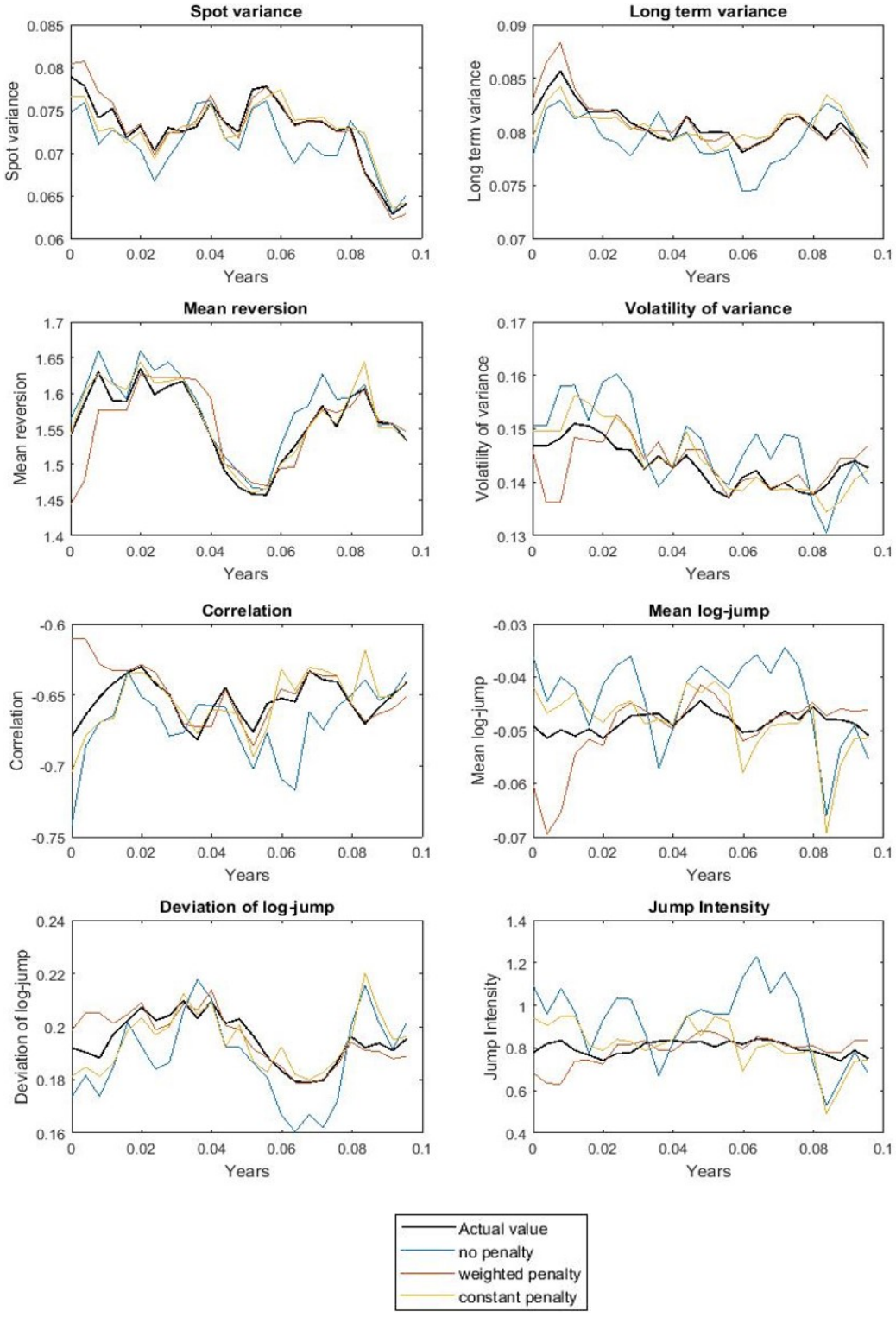

Fig. 6.1: Calibrated parameters for various choices of calibration penalty

Implied Volatility Calibration vs Option Price Calibration

Here calibration to call prices is compared to calibration to implied volatilities. In both cases, no penalty function is applied. It is clear from figure 6.2 that calibrating to implied volatilities produces a closer fit than calibration to call prices. However, calibration using implied volatilities took an average of 126 seconds, whereas the calibration to call prices took an average of 44 seconds. This is likely because of the extra step in the calibration of converting option prices to implied volatilities, which involves a root finding algorithm. This root finding algorithm is used inside a minimisation algorithm, which is likely the cause for the increased computational requirements.

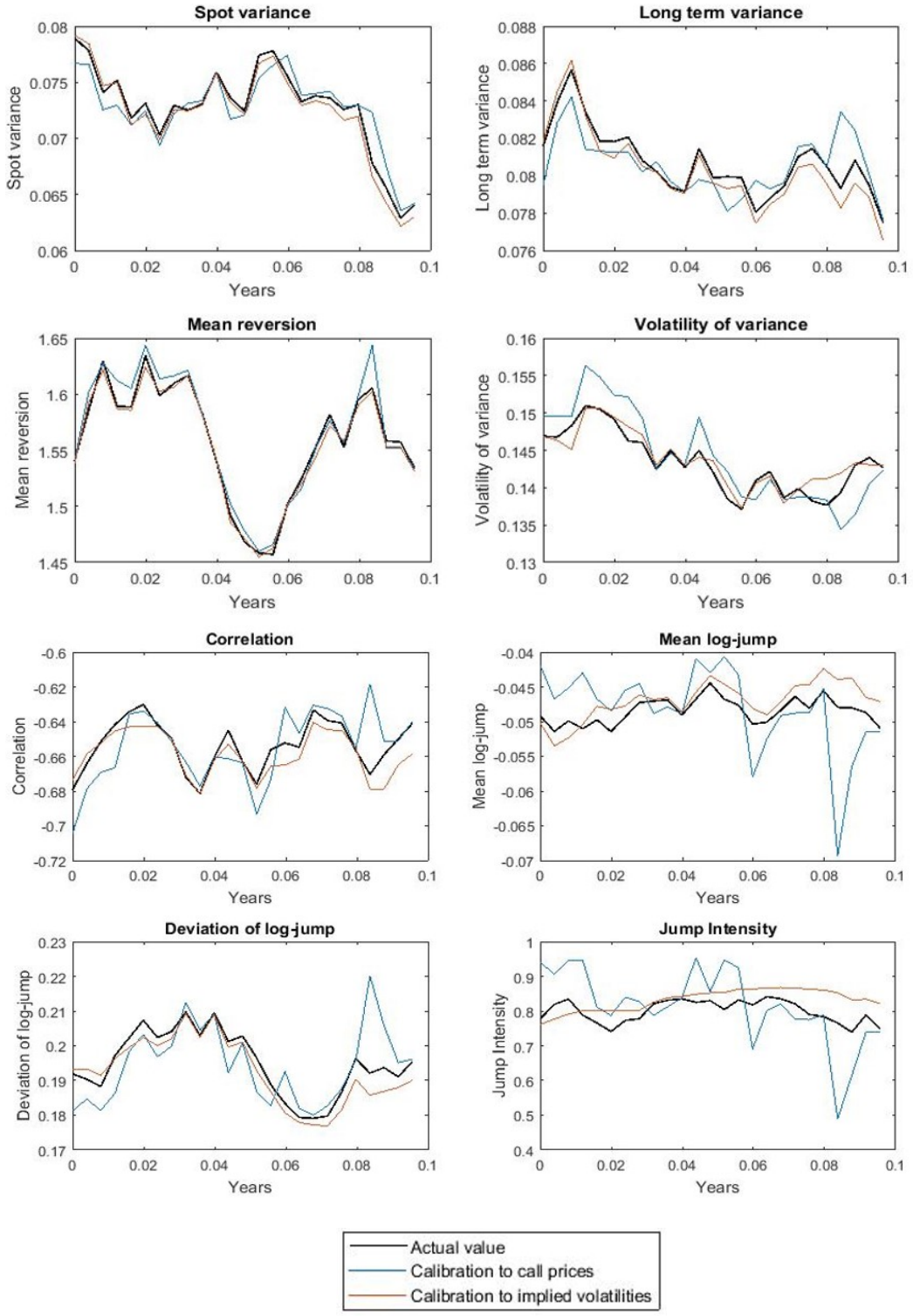

Fig. 6.2: Calibrated parameters using implied volatility or option prices as the calibration medium

6.2.2 Calibration with Varying Data Sets and Restrictions

This section investigates how much, and what type of data is required for adequate calibration. To display the difference between used data sets clearly, calibration to call prices with a constant penalty is used in all cases.

Restricted Strikes

As near the money options generally trade more liquidly, calibration can often face a limited range of strikes. The impact of the visible strike range is evaluated by using 3 sets of data with 7 strikes each, ranging between $\pm 10\%$, $\pm 30\%$ and $\pm 60\%$ moneyness respectively. Figure 6.3 proves that calibration of this sort is highly sensitive to strike range. The strikes ranging between $\pm 10\%$ give wildly varying parameters, despite the penalty used. The strikes ranging between $\pm 60\%$ however, recover the parameters and spot variance almost exactly.

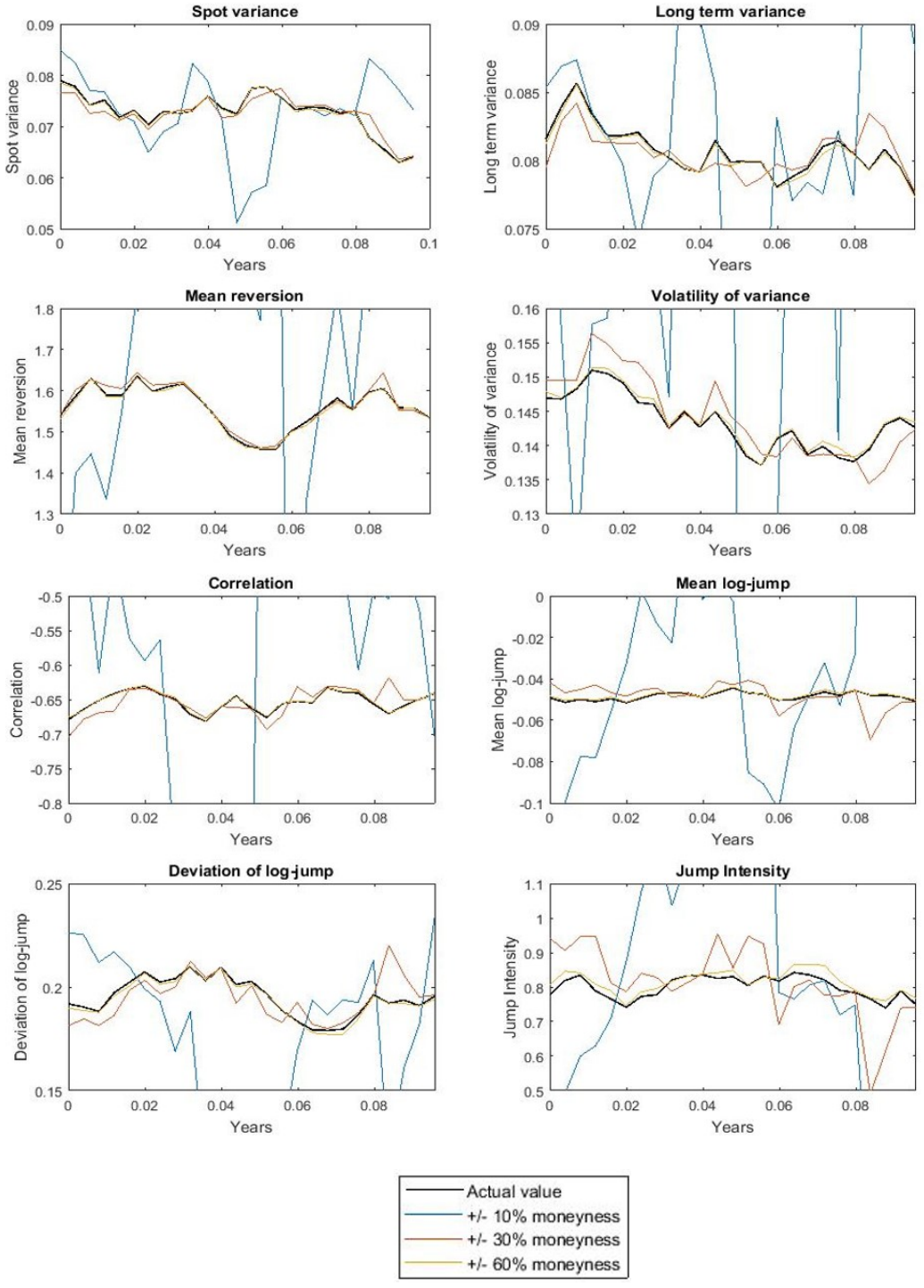

Fig. 6.3: Calibrated parameters using various ranges of observed strikes

Restricted Maturities

Due to liquid options generally having maturities of less than 2 years, calibration is often restricted to these shorter maturity options. Three different sets of data are used to investigate this effect. One set is chosen to be like the real world data in this study, and therefore consists of two maturities of 6 and 12 months. The second set has 4 maturities ranging between 6 months and 2 years. The final set considered has 6 maturities which range between 6 months and 10 years. As clearly visible in figure 6.4, the set of 2 maturities is by far inferior to the other two sets. Here, the link between volatility of variance and correlation is clear, with a large magnitude of correlation being compensated for by a low volatility of variance, and vice versa. Magnitude of correlation and mean reversion are also clearly linked, which further reduces the effect of the overestimated correlation factor. Interestingly however, there is not much difference between the set of 4 and 6 maturities. This implies that for the set of parameters chosen for simulation, the data given at the long end of the curve is redundant.

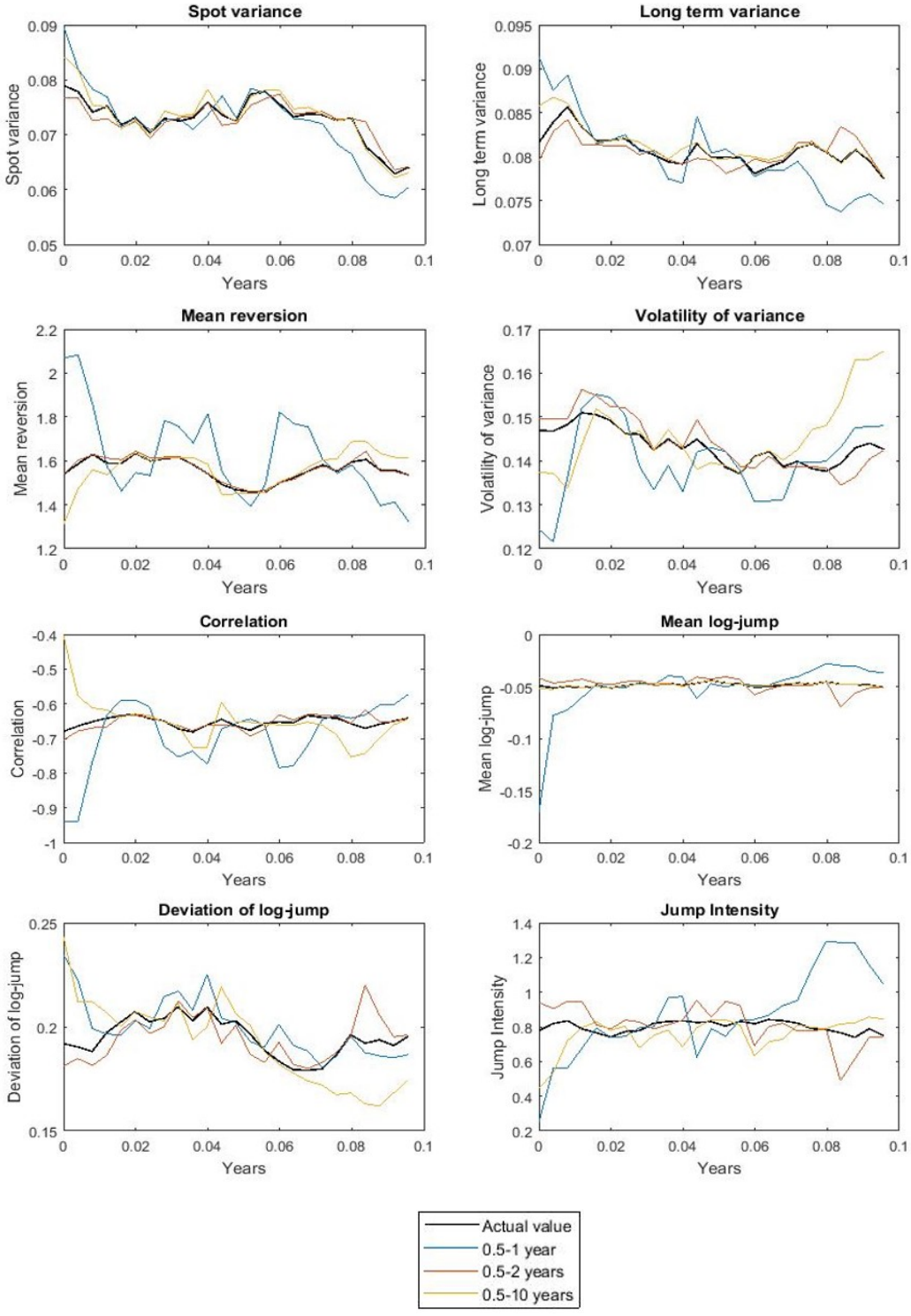

Fig. 6.4: Calibrated parameters using various ranges of observed maturities

6.2.3 Chosen Calibration, and Performance on Simulated Data

As a weighted penalty and calibration to implied volatilities perform the best, this type of calibration is chosen for simulated data. The resulting average RMSEs for various models are conveyed in table 6.1.

Tab. 6.1: Average RMSEs for calibration to simulated data

	Black-Scholes RMSE	Heston RMSE	Merton RMSE	Bates RMSE
Average	1.92	0.035	0.23	0

It is clear here that the fit of the calibrated Bates model to the input data is exact, even if the parameters do not exactly match the parameters used to simulate. This conveys the ability of the Bates model to fit a surface in several ways, using various combinations of parameters. The Black-Scholes model clearly falls short of the other models considered. The base model RMSEs convey that stochastic volatility is more important than jumps to fit a Bates surface of the kind simulated. However, this is likely unique to choice of simulation parameters, and possibly if jumps where emphasised, this would not apply.

6.2.4 Fit to Observed Prices and Volatilities

As the real world data is set 3 months apart, it is possible that the optimal parameters for consecutive surfaces are completely different. Therefore, the penalty is not included in the calibration to real world data. The resulting RMSEs are displayed in table 6.2, with the calibrated parameters in figure B.2. The Bates model always produces the closest fit, but does not fit the surfaces exactly. This implies that real world option prices have noise that cannot be fully explained by the Bates model. The Heston model performs slightly better than the Merton model, implying that the stochastic volatility component is more important for fit in this case. The Black-Scholes RMSE suggests that the observed implied volatility surfaces have more of a skew than the simulated implied volatility surfaces, as the average RMSE is over twice that of the simulated RMSE.

Tab. 6.2: RMSEs for calibration to real world data

Date	Black-Scholes RMSE	Heston RMSE	Merton RMSE	Bates RMSE
2015/12/31	5.61	0.51	0.91	0.48
2016/03/31	5.20	1.24	1.80	0.38
2016/06/30	5.31	0.93	1.84	0.44
2016/09/30	5.42	1.18	0.96	0.72
2016/12/30	3.43	1.28	0.51	0.50
2017/03/31	5.28	0.58	1.77	0.42
2017/06/30	5.13	0.43	1.40	0.43
2017/09/29	4.79	2.40	0.90	0.50
Average	5.02	1.07	1.26	0.48

Volatility surfaces for the dates highlighted are plotted against the fitted models to visually convey the fit and characteristics of the models in question. Figure 6.5 displays how the Heston model battles to fit surfaces with an emphasised smile, but have a good fit to flatter surfaces, that exhibit only a skew.

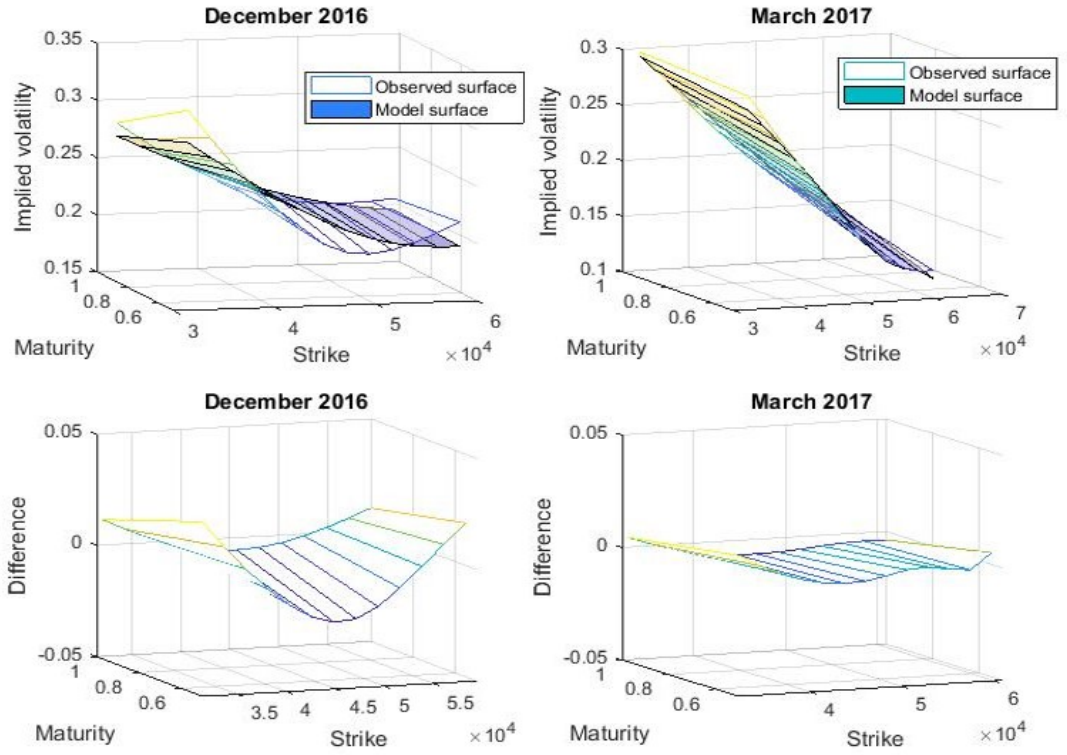

Fig. 6.5: Fitted Heston model

In contrast, the Merton model can be fitted to a short term smile fairly well, but battles to find parameters that fit both the front and back end of the flatter surface, as conveyed by figure 6.6.

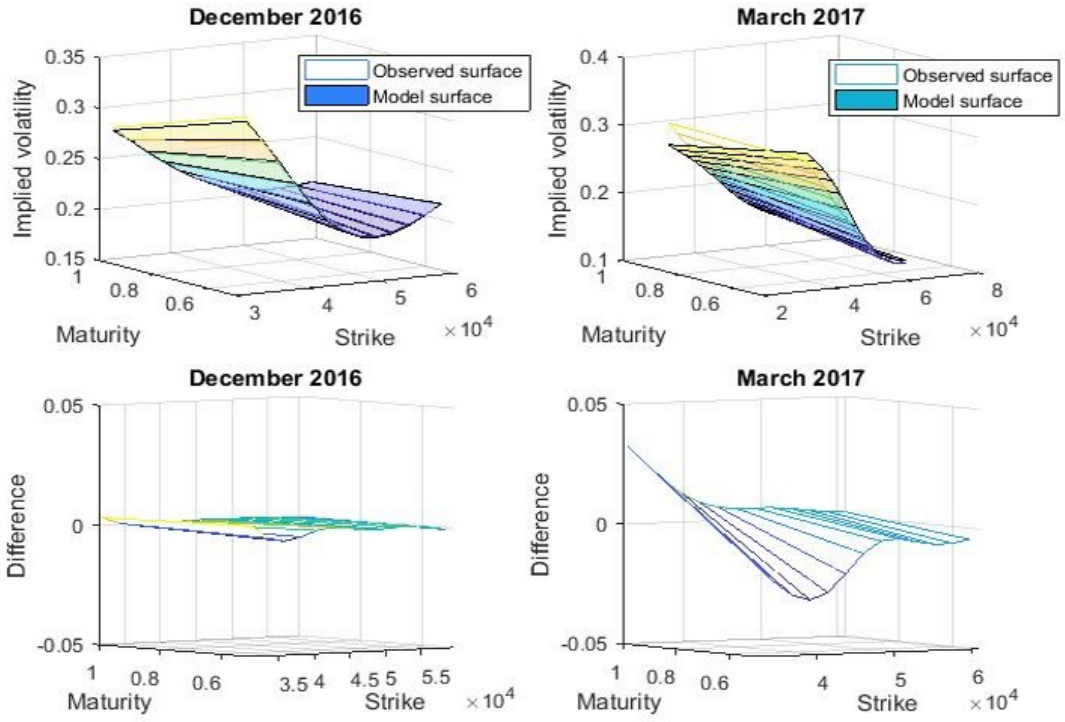

Fig. 6.6: Fitted Merton model

As the Bates model has the flexibility to combine the characteristics of these two models, figure 6.7 depicts a good performance for both dates. However, it is clear that the surfaces do not fit exactly.

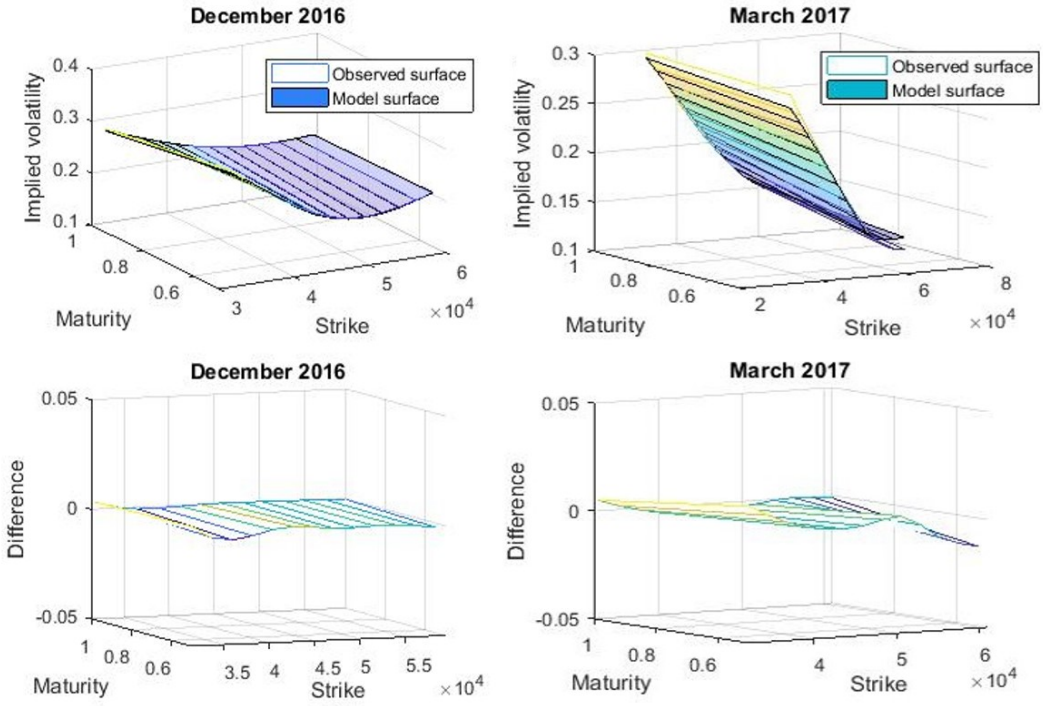

Fig. 6.7: Fitted Bates model

6.2.5 Out of Sample Fit

The out of sample fit of these models is tested by calibrating to option prices of the previous available date, and using these calibrated parameters to produce volatility surfaces on the current date by changing only the state processes and option strikes. The resulting RMSEs are displayed in table 6.3. This tests the stability of the model, as if the parameters are stationary, the model should fit equally as well. This would imply that the dynamics of the state processes have been properly captured in the previous calibration. However, in this case the RMSEs all increase, with the average Bates RMSE tripling. The Heston model is more stable, with an increase of only 50% and the Merton model doubles its RMSE. However, these results do not necessarily indicate the stability of the model overall, but rather the stability of the model when calibrated to limited data. Section 6.2.2 conveys that having only two maturities of 6 and 12 months is insufficient to recover parameters of simulated Bates data. It is therefore unsurprising that the out of sample Bates RMSE increases heavily.

Tab. 6.3: Out of sample RMSEs for calibration to real world data

Date	Black-Scholes RMSE	Heston RMSE	Merton RMSE	Bates RMSE
2016/03/31	5.27	0.96	1.24	1.06
2016/06/30	5.69	0.58	2.06	0.69
2016/09/30	6.08	1.16	3.16	1.37
2016/12/30	3.89	2.70	3.26	2.22
2017/03/31	5.96	2.45	3.96	3.61
2017/06/30	5.17	0.72	1.62	0.53
2017/09/29	5.77	3.05	3.41	1.31
Average	5.41	1.66	2.67	1.54

6.3 Hedging

6.3.1 Delta Hedging Using Only the Underlying

The leftmost graph in figure 6.8 displays two AAE surfaces for a delta hedge using just the underlying. One surface represents a Bates hedge, and the other a Black-Scholes hedge. For an at the money option, the AAE is about 1% of the option value. In both cases, the AAE is high for close to the money short maturity options. As the maturity of the option grows, so does the AAE, which is likely because of the higher cost associated with longer maturity options. These two surfaces seem indistinguishable, despite the option values and state processes being generated in a Bates type setting. The Black-Scholes AAE is subtracted from the Bates AAE in the rightmost graph. A positive difference would imply that the Bates model on average gives a daily hedge error of smaller magnitude than the Black-Scholes model. This is the case for most of the surface, with short maturity near the money options being the exception. The Bates model appears to perform significantly better than the Black-Scholes model for away from the money short term options. However, the improvement in performance of the Bates model for hedging long maturity options is small, giving a reduction of about 1% in AAE. Although this may seem surprising, section 3 demonstrates how similar the deltas are for the two different models under the chosen base parameters.

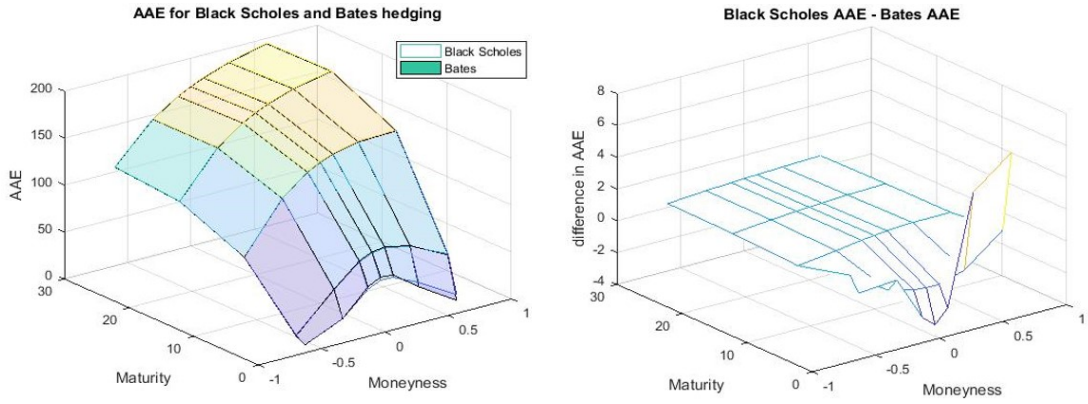

Fig. 6.8: Comparison of Black-Scholes and Bates AAEs for a delta hedge

Figure 6.9 conveys that the hedging biases for the two different models are also similar. The difference between hedging bias displayed in the rightmost graph of this figure shows that hedging using the Black-Scholes model for short maturity near the money options gives significantly more bias, which accounts for the slightly lower AAE. The likely explanation for the low AAE and high HB is that the overestimated delta at short maturities near the money (as is apparent in figure 3.1) helps mitigate some of the gamma risk, but leads to exaggerated hedge bias. There is not a significant difference in HB for away from the money short maturity options, implying that the Bates model results in a less volatile hedge with no increase in bias for these types of options. As the HB value in essence gives the bias for the hedge of a long call, it is realistic that this value is always positive, as the gamma of the option will always result in it performing better than the hedge portfolio. This is due to the value of the hedge portfolio only moving linearly with stock price, whereas the option value has a non-linear relationship.

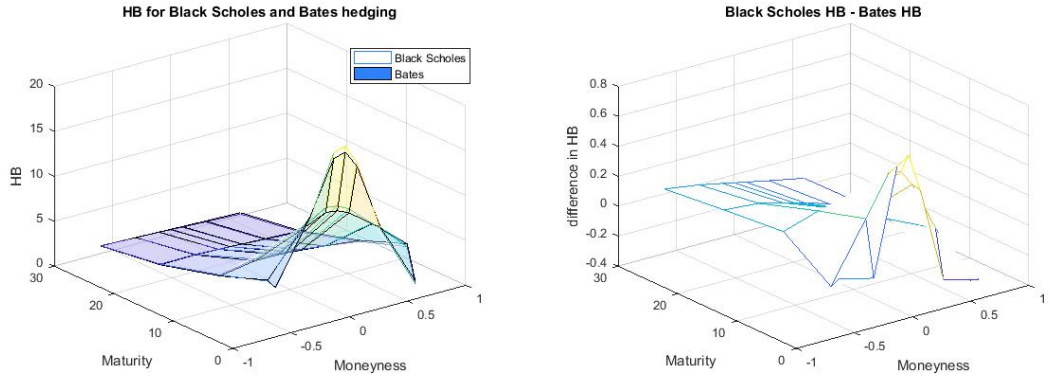

Fig. 6.9: Comparison of Black Scholes and Bates HBs for a delta hedge

The performance of the Heston model as depicted by the leftmost graph in figure 6.10 is almost equivalent to the Bates model. The rightmost graph shows that there is more difference in the short term hedge between the Merton and Bates models. This is consistent with the RMSE values in table 6.1, that show for the chosen parameters, the Heston model fits the Bates produced surface better than the Merton model. The weak performance of the Merton model for short maturity options is surprising, but is possibly due to the model overcompensating in an attempt to fit the back end of the surface.

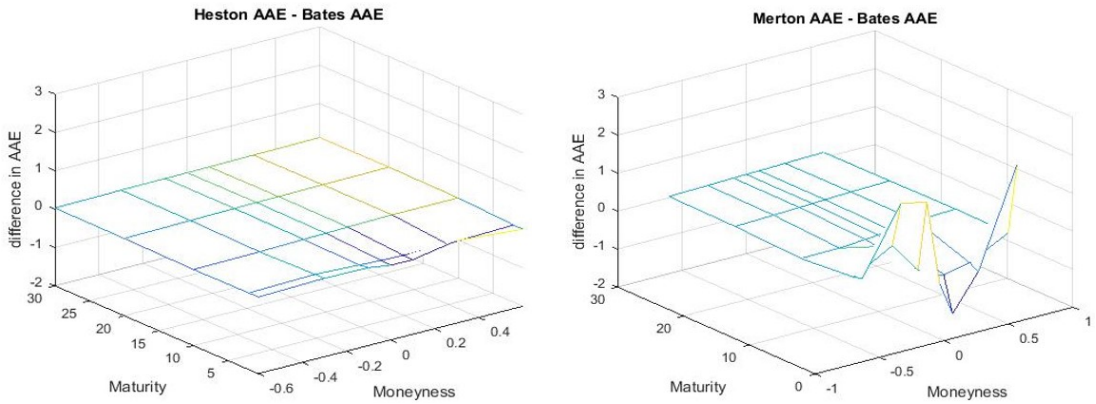

Fig. 6.10: Comparison of Bates AAEs to Heston and Merton AAEs for a delta hedge

As conveyed in figure 6.11 the LV model outperforms the Black Scholes model, especially for longer maturities. It should be noted however that the LV model is extremely sensitive to visible range of options, and therefore it cannot be concluded

that this will always be the case.

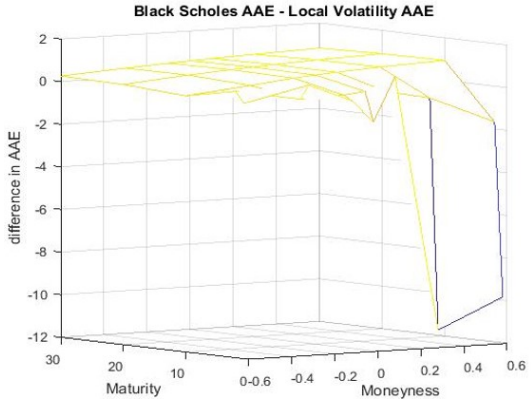

Fig. 6.11: Comparison of Black-Scholes AAEs to LV for a delta hedge

Under this setting, the LV model performs equally as well as the Bates model for hedging long term options using the underlying, even producing a slightly lower hedging bias then the Bates equivalent. However, it does not perform as well for hedging short term options.

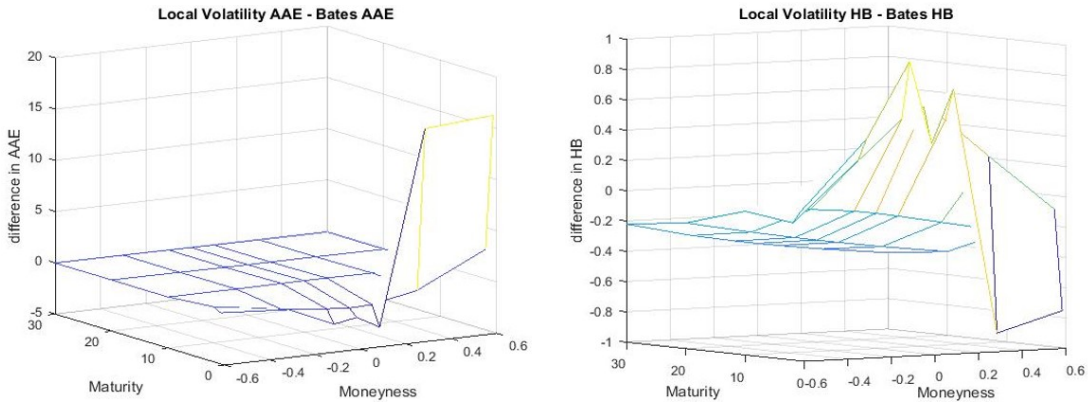

Fig. 6.12: Comparison of Bates and LV AAEs and HBs for a delta hedge

To conclude this section, it must be emphasised that these results apply to the chosen simulated setting. If parameters that cause larger differences in delta values were chosen for simulation (see section 3), then it is likely that the difference in hedging between Black-Scholes and Bates would be more stark. However, investigation of this is left to further studies.

6.3.2 Delta and Vega Hedging

Figure 6.13 displays the result of a delta and vega hedge on the simulated data, using the Black-Scholes and Bates models. The leftmost graph clearly shows that the AAE is much lower for this type of hedge compared to a delta hedge. This hedge also has less of an increase in AAE when hedging long maturity options. There is a depression in the AAE at about 10% in the money at a 1 year maturity, which is due to the option being used in the hedge portfolio having a moneyness of 15% and maturity of 1.2 years. This similarity in moneyness and maturity means that the options will have similar sensitivities to both the underlying and volatility, and therefore the hedge portfolio is more likely to have a similar performance to the hedged instrument. In this case, the difference in performance between the Black-Scholes model and the Bates model is clear, with the Bates model performing better at every point on the surface. As is clear from the rightmost graph, the AAE on the long end of the surface is about 15% lower for the Bates hedge compared to the Black-Scholes hedge. This difference in hedging result is likely because of the different volatility assumptions of the models.

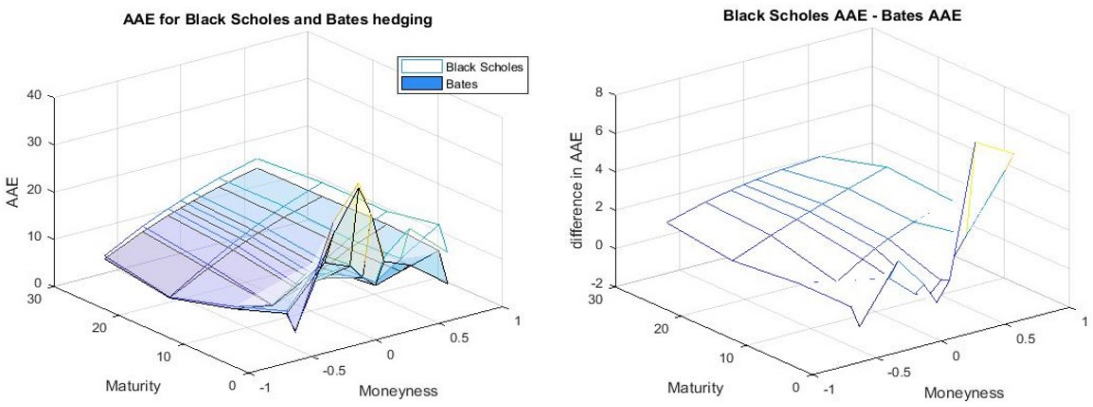

Fig. 6.13: Comparison of Black Scholes and Bates AAEs for a delta-vega hedge

A vega hedge, which involves holding an option in the hedge portfolio, involves removing some of the gamma risk. This is clear from the HB surfaces displayed in figure 6.14, as the hedging bias is no longer always positive, and is close to 0 on the long end of the surface. There is a spike in hedging bias close to the money for short maturity options.

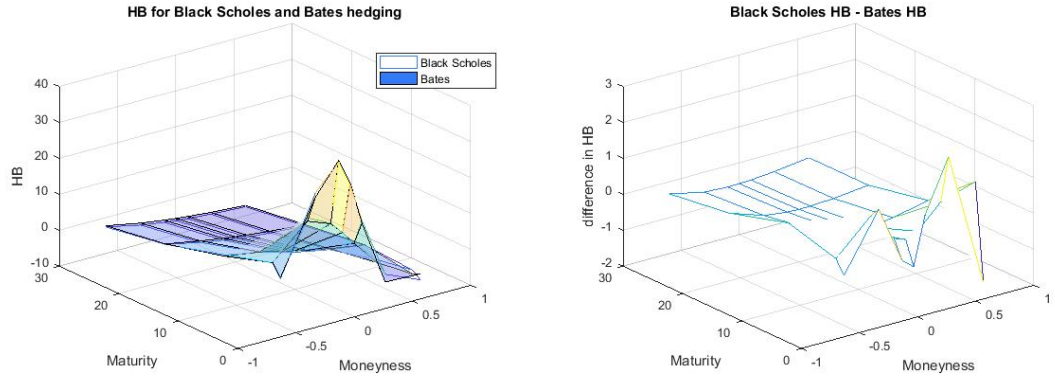

Fig. 6.14: Comparison of Black-Scholes and Bates HBs for a delta-vega hedge

Figure 6.15 conveys the performance of the base models relative to the Bates model. The leftmost graph suggests that the Heston and Bates models have very similar performances in this setting. The Merton model, although better than the Black-Scholes model, is clearly worse than the Heston model. This indicates that stochastic volatility is the more important for vega hedging in this setting, which again, is likely a consequence of different assumptions around the volatility of the underlying.

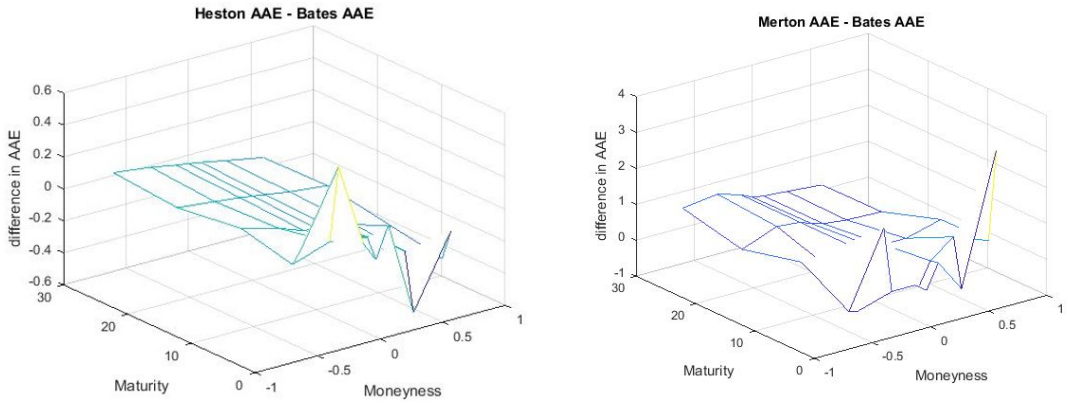

Fig. 6.15: Comparison of Bates AAEs to Heston and Merton AAEs for a delta-vega hedge

As is clear from figure 6.16, there is no significant improvement using the LV model compared to Black-Scholes model. Therefore, local volatility models are not considered further for delta-vega hedging.

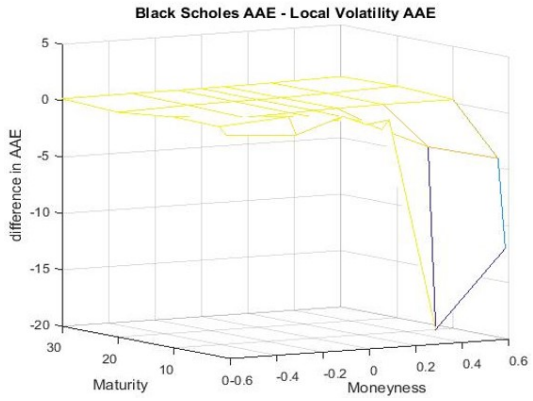

Fig. 6.16: Comparison of Black-Scholes and LV AAEs for a delta-vega hedge

Chapter 7

Conclusion

Challenges around risk-neutral calibration of the Bates model have been thoroughly assessed in a simulated environment. Investigation into different types of calibration have displayed that an implied volatility loss function performs better than an option price loss function. The addition of a penalty term was shown to reduce parameter volatility, and lead to enhanced parameter recovery in the chosen simulated environment. Calibration under different data restrictions showed that a large range of strikes is important for parameter recovery. Although two maturities were insufficient for calibration, the liquid range was shown to be sufficient for the chosen setting. In the context of a potentially illiquid market, this discourages the use of the Bates model when there is a lack of visible data. Regardless of available data however, the Bates model achieves a superior fit to the JSE Top 40 Equity Index implied volatility surfaces when compared to its base models, re-enforcing the conclusion of previous authors that both jumps and stochastic volatility are necessary additions for no-arbitrage pricing.

Under modest base parameters in the simulated setting, the Bates model did not greatly improve delta hedging performance, even when option prices and state processes were simulated using Bates dynamics. This is especially true for options with a long maturity, conveying that use of the Bates model for long term hedging is not always necessary, as more parsimonious models perform equally well. However, under more extreme parameters it is unlikely that this conclusion will hold, due to the accentuated differences in delta values found for certain parameter combinations. Further study in this area is recommended, in order to clarify if there are surfaces where the Bates model is superior, and if so, how to identify these surfaces. The investigation into delta and vega hedging, using a portfolio of the underlying and an additional option, reached a different conclusion. Even under modest parameters, the Bates model clearly outperformed the Black-Scholes and local volatility models. However, under the chosen simulation, the Heston model

performed equally well, implying that the addition of jumps may not always be necessary for a delta-vega hedge.

Bibliography

Andersen, T. G., Benzoni, L. and Lund, J. (2002). An empirical investigation of continuous-time equity return models, *The Journal of Finance* **57**(3): 1239–1284.

Bakshi, G., Cao, C. and Chen, Z. (1997). Empirical performance of alternative option pricing models, *The Journal of Finance* **52**(5): 2003–2049.

Bates, D. S. (1996). Jumps and stochastic volatility: Exchange rate processes implicit in deutsche mark options, *The Review of Financial Studies* **9**(1): 69–107.

Bates, D. S. (2000). Post-'87 crash fears in the s&p 500 futures option market, *Journal of Econometrics* **94**(1-2): 181–238.

Bates, D. S. (2003). Empirical option pricing: A retrospection, *Journal of Econometrics* **116**(1): 387–404.

Bekaert, G. and Harvey, C. R. (1997). Emerging equity market volatility, *Journal of Financial economics* **43**(1): 29–77.

Black, F. and Scholes, M. (1973). The pricing of options and corporate liabilities, *Journal of political economy* **81**(3): 637–654.

Chernov, M., Gallant, A. R., Ghysels, E. and Tauchen, G. (2003). Alternative models for stock price dynamics, *Journal of Econometrics* **116**(1): 225–257.

Cont, R., Tankov, P. and Voltchkova, E. (2004). Option pricing models with jumps: integro-differential equations and inverse problems.

Demirgüç-Kunt, A. and Levine, R. (1996). Stock market development and financial intermediaries: stylized facts, *The World Bank Economic Review* **10**(2): 291–321.

Gatheral, J. (2011). *The volatility surface: a practitioner's guide*, Vol. 357, John Wiley & Sons.

Heston, S. L. (1993). A closed-form solution for options with stochastic volatility with applications to bond and currency options, *The review of financial studies* **6**(2): 327–343.

Kienitz, J. and Wetterau, D. (2012). *Financial modelling: Theory, implementation and practice with MATLAB source*, John Wiley & Sons.

Merton, R. C. (1976). Option pricing when underlying stock returns are discontinuous, *Journal of financial economics* **3**(1-2): 125–144.

Møller, T. (2001). Hedging equity-linked life insurance contracts, *North American Actuarial Journal* **5**(2): 79–95.

Appendix A

Option Pricing and Local Volatility Models

A.1 Option Pricing Formulae and Theorems

A.1.1 Pricing Vanilla European Options using Direct Integration of the Gil-Pelaez Inversion Theorem

The Gil-Pelaez Theorem states:

Theorem A.1. *Let $F(x) := \mathbb{P}(X \leq x)$ be the distribution function of a random variable X (which need not have a density function), and let $\varphi(\theta) := \mathbb{E}[e^{i\theta X}]$ be its characteristic function. Then:*

$$\mathbb{P}(X \geq x) = \frac{1}{2} + \frac{1}{\pi}\int_0^\infty Re\left(\frac{e^{-i\theta x}\varphi(\theta)}{i\theta}\right)\mathrm{d}\theta \tag{A.1}$$

Denote the bank account by $A_t := e^{\int_0^t r_u \mathrm{d}u}$ and let $\mathbb{Q}$ be the risk neutral measure. Let $\mathbb{Q}^T$ be the EMM for the bond numéraire, $P(t,T)$ and let $\mathbb{Q}_S$ be the EMM for the stock price numéraire, S_t. The price of a Vanilla European Option can be written as the expectation under the risk neutral measure of the discounted payoff. Consider a European Call $C(t,S_t)$ with strike K and maturity T. The $t = 0$ price can be written as

$$\begin{aligned} C(0,S_0) &= A_0\mathbb{E}\left[\frac{(S_T-K)^+}{A_T}\right] \\ &= S_0\mathbb{Q}_S(S_T \geq K) - KP(0,T)\mathbb{Q}^T(S_T \geq K) \end{aligned} \tag{A.2}$$

Define $X_T = \ln S_T$ and let $\phi(\theta)$ and $\varphi(\theta)$ be characteristic functions of X_T under $\mathbb{Q}^T$ and $\mathbb{Q}_S$ respectively.

$$\phi(\theta) := \mathbb{E}_{\mathbb{Q}^T}[e^{i\theta X_T}] \quad \varphi(\theta) := \mathbb{E}_{\mathbb{Q}_S}[e^{i\theta X_T}]$$

Observe that

$$\begin{aligned} \varphi(\theta) &= \mathbb{E}_{\mathbb{Q}_S}[e^{i\theta X_T}] \\ &= \mathbb{E}_{\mathbb{Q}^T}\left[e^{i\theta X_T}\frac{d\mathbb{Q}_S}{d\mathbb{Q}^T}\right] \\ &= \frac{P(0,T)}{S_0}\mathbb{E}_{\mathbb{Q}^T}\left[e^{i\theta X_T}S_T\right] \end{aligned}$$

Since $(S_t/P(t,T))_t$ is a $\mathbb{Q}^T$ martingale,

$$\frac{S_0}{P(0,T)} = \mathbb{E}_{\mathbb{Q}^T}\left[\frac{S_T}{P(T,T)}\right] = \mathbb{E}_{\mathbb{Q}^T}\left[e^{X_T}\right] = \mathbb{E}_{\mathbb{Q}^T}\left[e^{i(-iX_T)}\right] = \phi(-i)$$

Therefore

$$\varphi(\theta) = \frac{P(0,T)}{S_0}\mathbb{E}_{\mathbb{Q}^T}\left[e^{i\theta X_T}S_T\right] = \frac{\mathbb{E}_{\mathbb{Q}^T}\left[e^{i(\theta-i)X_T}\right]}{\phi(-i)} = \frac{\phi(\theta-i)}{\phi(-i)}$$

Now the price of a call price can be written as a function of the characteristic function of X_T under $\mathbb{Q}^T$ as per equations (A.4) and (A.3).

$$Q_j = \frac{1}{2} + \frac{1}{\pi}\int_0^\infty Re\left(\frac{e^{-i\theta x}\phi(\theta - ij)}{i\theta\phi(-ij)}\right)\mathrm{d}\theta \qquad for \quad j = 0,1 \tag{A.3}$$

$$C(0,S_0) = S_0Q_1 - P(0,T)Q_0 \tag{A.4}$$

A.2 Characteristic Functions

A.2.1 Heston Characteristic Function

The risk-neutral little trap formulation of the Heston characteristic function is displayed below. The little trap formulation allows for better integrability than the original provided by Heston (1993).

$$\varphi_H(u,t,T) = \exp(A_H(u,t,T) + B_\sigma(u,t,T)v_t + i\,u\,(\ln(S_t) + (r-d)(T-t))) \tag{A.5}$$

with

$$\begin{aligned}
A_H(u,t,T) &= \frac{\kappa\overline{v}}{\sigma^2}\left((\kappa - \rho\sigma u\, i - D)(T-t) - 2\log\left(\frac{G\exp(-D(T-t))}{G-1} - 1\right)\right)\\
B_\sigma(u,t,T) &= \frac{\kappa - \rho\sigma u\, i - D}{\sigma^2}\left(\frac{1-\exp(-D(T-t))}{1 - G\exp(-D(T-t))}\right)\\
G &= \frac{\kappa - \rho\sigma u\, i - D}{\kappa - \rho\sigma u\, i + D}\\
D &= \sqrt{(\kappa - \rho\sigma u\, i)^2 + u(i+u)\sigma^2}
\end{aligned}$$

A.2.2 Merton Characteristic Function

The risk-neutral Merton Characteristic function is given below.

$$\varphi_M(u,t,T) = \exp\left((T-t)\lambda\left[\exp\left(i\mu_j u - \frac{\sigma_j^2u^2}{2}\right) - 1\right] + iu\left[\ln(S_t) + \left(r - d - \frac{1}{2}\overline{v} - \lambda k\right)(T-t)\right] - \frac{\overline{v}u^2}{2}(T-t)\right) \tag{A.6}$$

where k is the expected magnitude of the jump, given by

$$k = \exp\left(\mu_j + \frac{1}{2}\sigma_j^2\right) - 1$$

A.2.3 Bates Characteristic Function

The risk-neutral Bates characteristic function is given below. This characteristic function takes the drift and volatility components from the Heston Characteristic function A.5, and the jump component from the Merton Characteristic function A.6. Again, using the little trap formulation for the Heston Characteristic function improves integrability.

$$\varphi_B(u,t,T) = \varphi_H(u,t,T)\exp\left((T-t)\lambda\left[\exp\left(i\mu_j u - \frac{\sigma_j^2 u^2}{2}\right)-1\right]-iu\lambda k(T-t)\right) \quad \text{(A.7)}$$

A.3 Local Volatility Models

These models use observed option prices to set a unique volatility for each combination of strike and maturity. These models assume that the local volatility surface is static.

A.3.1 Dupire Volatility

The form of a Black-Scholes risk-neutral Dupire local volatility model is displayed in equation (A.8).

$$\frac{\mathrm{d}S_t}{S_t} = (r-d)\mathrm{d}t + \sigma(S_t,t)\mathrm{d}Z_t \quad \text{(A.8)}$$

where $\sigma(S_t,t)$ is the Dupire volatility obtained from observed option price surface using equation (A.9)

$$\sigma(K,T,S_t) = \sqrt{\frac{\frac{\delta X}{\delta T}}{\frac{1}{2}K^2\frac{\delta^2 X}{\delta K^2}}} \quad \text{(A.9)}$$

Here, X is the observed price of a European put or call at time t with strike K and maturity T. It must be noted that this equation requires the computation of derivatives at the points in question, and is therefore sensitive to the method used, as well as the availability of data. Finite difference is commonly used in practice, and will therefore be implemented for this model. In the case of simulated data, although the implied volatility surface is known at any point, only chosen visible points are used for finite difference, as this is a better representation of reality.

Appendix B

Additional Data, Results and Analysis

B.1 Base Bates Parameters

The chosen base parameters are based loosely off those presented by Bakshi *et al.* (1997) who calibrated to S&P 500 options. The long term volatility and the initial volatility where chosen to be slightly higher, to account for the higher level of volatility experienced in developing markets. The stock price was chosen to be 100.

Tab. B.1: Base scenario parameters

Parameter	Base Value
S_0	100
v_0	0.08
r	0.06
d	0.01
ρ	-0.6
$\overline{v}$	0.07
σ	0.15
κ	1.5
μ_j	-0.05
σ_j	0.2
λ	0.6

B.2 Comparison of Monte Carlo Prices to Gil-Pelaez Prices

Figure B.1 conveys the difference in prices between the Gil-Pelaez and Monte Carlo prices computed using the base model parameters and state variables in table B.1. The leftmost graph in this figure gives the indication that the prices may converge, but as the number of samples is increased, it becomes clear that longer maturity options have a fairly significant biased. This is due to the discretisation becoming more bias as the simulation becomes longer.

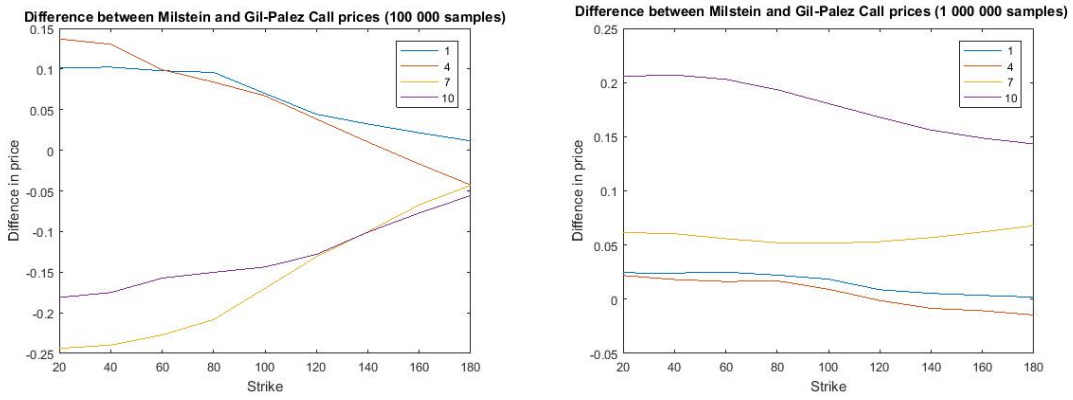

Fig. B.1: Difference between Milstein and Gil-Palez call prices for different maturities and strikes

B.3 Bootstrapping Data

As only short maturity options are visible in typical option data, calibration for pricing long term options can challenging. A typical two parameter model used to extrapolate implied volatility is detailed in equation (B.1).

$$IV^{MODEL}(T) = \sqrt{(IV_\infty)^2 + \frac{1}{\alpha T}(1 - e^{-\alpha T})((IV_0)^2 - (IV_\infty)^2)} \tag{B.1}$$

Here α and IV_∞ must be calibrated, whereas IV_0 is the implied volatility of the shortest visible options. This model can be calibrated using the same form of equation (4.4). Whether this method of bootstrapping data adds value to calibration is unclear.

Considering the provided data contains only 2 maturities, which as seen in section 6.2.2, introduces problems into calibration, it would be helpful if bootstrapping data was a viable option. Equation (B.1) is therefore used to bootstrap simulated data from 2 maturities to 4 maturities. The Bates model calibrated using 2 maturities is used to do the same thing in order to access performance. The RMSE between the bootstrapped surface and the actual surface is calculated for both methods, resulting in an average RMSE of 7.8×10^{-6} for the bootstrapping method and 5.2525×10^{-9} for the Bates model. Although it is therefore clear the Bates model performs better with simulated data, this will not necessarily hold with market data, as an exact fit of the Bates model to market data is not always possible. However, market data with more than 2 maturities would be required to test this method, and therefore this is left to further studies.

B.4 Equity-linked Endowment Contract

In order to make the long term hedging study more applicable to industry, the instrument chosen is a call option. This is due to its similarity to a equity-linked pure endowment contract. These contracts obligate the insurer to pay the policy holder the maximum of a fixed value and certain amount of a stock index either when the policy holder dies, or when the contract expires. These contracts are exposed to the index, and the time of mortality of the policy holder. However, Møller (2001) suggests using the expected course of the policy holders life due to insurers typically holding a large amount of contracts, claiming this can be justified using the law of large numbers. Assuming this is true, the payoff of this contract ($\mathcal{F}$) can be described by equation (B.2).

$$\begin{aligned} \mathcal{F} &= \max(S_T, K) \\ &= K + \max(S_T - K, 0) \end{aligned} \tag{B.2}$$

Therefore, the policy, from and insurers perspective, collapses to some amount of short vanilla calls on an index and a fixed payment of cash. The cash does not effect the choice of security price model used pricing or hedging, and can therefore be ignored. The number of calls is a matter of multiplication, and therefore it is assumed that the policy involves one call. Usually, these contracts obligate the policy holder to pay premiums throughout the life of the contract, rather than a once off payment at the initiation of the contract. However, as we assume a constant interest rate and a European style maturity, it is a simple matter to discount all future payments to the initiation date. These simplifications do not detract from the analysis of the different models, as predicting yield curves and mortality risk are not dependent on the choice of security price model. These instruments typically are offered with maturities of 10-30 years.

B.5 Bates Empirical Calibrated Parameters

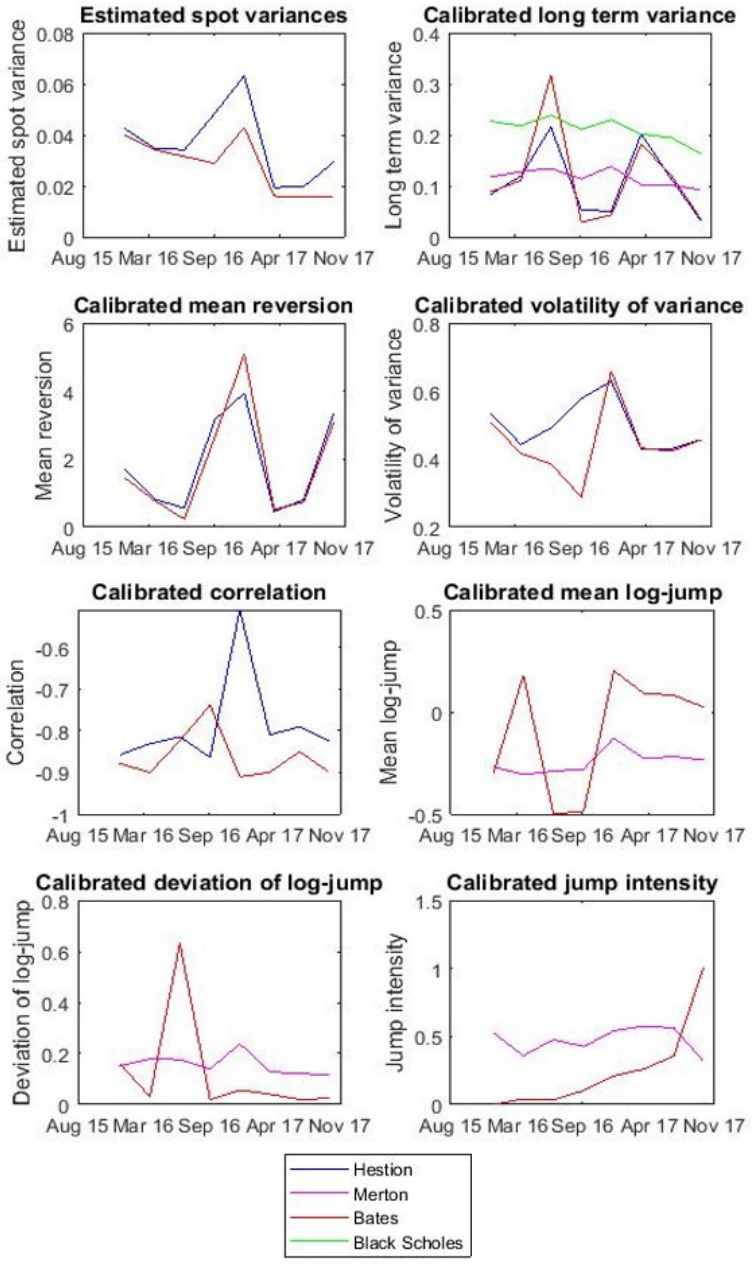

Fig. B.2: Calibrated parameters using various ranges of observed maturities

B.6 Convergence of Hedging Measures

In order to ensure the chosen measures are stable enough for analysis, their behaviour for different amounts of input data were tracked. The input data used was the simulated data from the hedging analysis (see section 5.2). The x-axes in figure B.3 corresponds to the number of days contributing to the AAE and HB respectively. Figure B.3 conveys how the HB oscillates at first, but converges to a stable value. The AAE on the other hand does not appear to converge to a single value, but is reasonably stable. This lack of convergence is likely due to the stochastic variance. Periods of higher volatility would result in larger hedge errors, and vice versa for low volatility periods. This would effect the AAE value, pushing it up for high volatility periods. However, this effect would affect all models in the same manner, and therefore still allows for comparison. The HB is reasonably unaffected, as high volatility periods would not change the bias of the hedge.

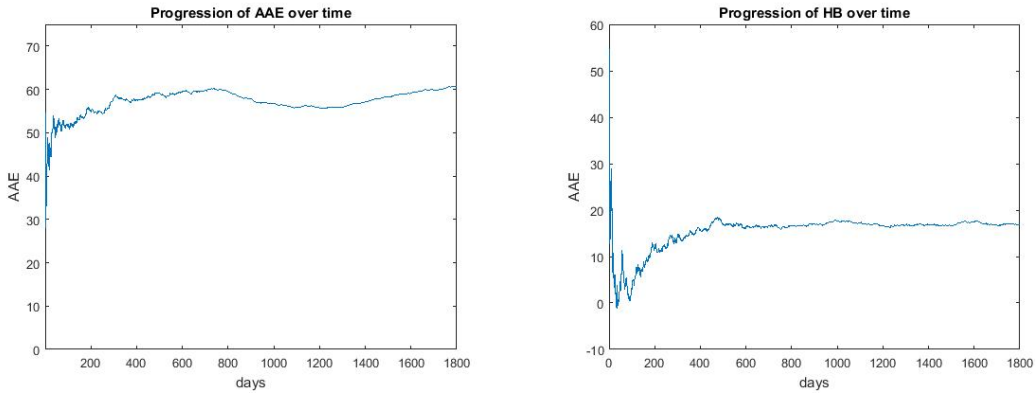

Fig. B.3: Convergence of hedging measures